Supplement of Atmos. Chem. Phys., 18, 17819–17841, 2018
https://doi.org/10.5194/acp-18-17819-2018-supplement

Atmospheric Chemistry and Physics
Open Access
EGU

Supplement of

Principal component analysis of summertime ground site measurements in the Athabasca oil sands with a focus on analytically unresolved intermediate-volatility organic compounds

Travis W. Tokarek et al.

Correspondence to: Hans D. Osthoff (hosthoff@ucalgary.ca)

Table of contents

Descriptions of instrumentation used

A Griffin 450 gas chromatograph equipped with a cylindrical ion trap mass spectrometer and electron impact ionization (GC-ITMS) was used to quantify selected VOCs including o-xylene, decane, undecane, 1,2,3- and 1,2,4-trimethylbenzene (TMB), and several monoterpenes (i.e., α-pinene, ß-pinene and limonene). The GC-ITMS primary responsibility was the quantification of monoterpenes. The remaining VOCs quantified were chosen because (a) they sufficiently resolved on the analytical column, and (b) response factors could be determined, either because the compounds of interest were part of the VOC standard used in the field (such as the aromatics o-xylene, 1,2,3- and 1,2,4-TMB, see below) or relative response factors were determined post-campaign. Operation, calibration and performance of this instrument have been described elsewhere (Tokarek et al., 2017; Liggio et al., 2016). Briefly, the GC was operated with 30 m (length) × 0.25 mm (inner diameter) × 0.25 µm (film thickness) DB-5MS analytical column with helium carrier gas. The GC-ITMS sampled from a 3.6 m long stainless-steel inlet with an o.d. of 0.635 cm from a height of 5 m above ground. A 1 m long section of the inlet was heated to 110 °C and optimized to remove interference due to O_3 while avoiding decomposition of alkenes (Tokarek et al., 2017). The GC oven was programmed as follows: hold at 40 °C for 3.00 min, heat at 1.5 °C min^{-1} to 70° C (reached at 23.00 min), heat at 5° C min^{-1} to 200 °C (reached at 49.00 min) and hold for 4 min (total 53.00 min). This was followed by a 5 min recovery time to allow the oven and pre-concentration trap to cool back to 40 °C. The ion trap mass spectrometer was set to an *m/z* range of 50-425. After data reduction, the GC-ITMS generated 10-minute average concentrations of each VOC quantified every hour.

During the campaign, the GC-ITMS was calibrated in the field using an IONICON VOC standard (Table S-1) containing (in addition to VOCs that the GC-ITMS did not detect) α-pinene and o-xylene at mixing ratios of ~ 1 ppmv and an uncertainty of 5% and 6%, respectively. A commercial calibrator assembly (IONICON, GCU Standard) was used to deliver diluted calibration mixtures. The instrument responses to

the VOC standards were linear ($R^2 > 0.99$). The GC-ITMS was calibrated for other VOCs offline relative to α-pinene. In the field, there was no noticeable carry-over (i.e., memory effects) of IVOCs, which was occasionally evaluated by flooding the inlet with purified, VOC-free air.

Matrices of ions plotted against retention times for the total ion chromatograms (shown in Figure 2 in the main manuscript) are shown in Fig. S-1. In both cases, the greatest intensity is with masses are associated with alkanes (i.e., *m/z* 55, 57, 67, 69, etc.).

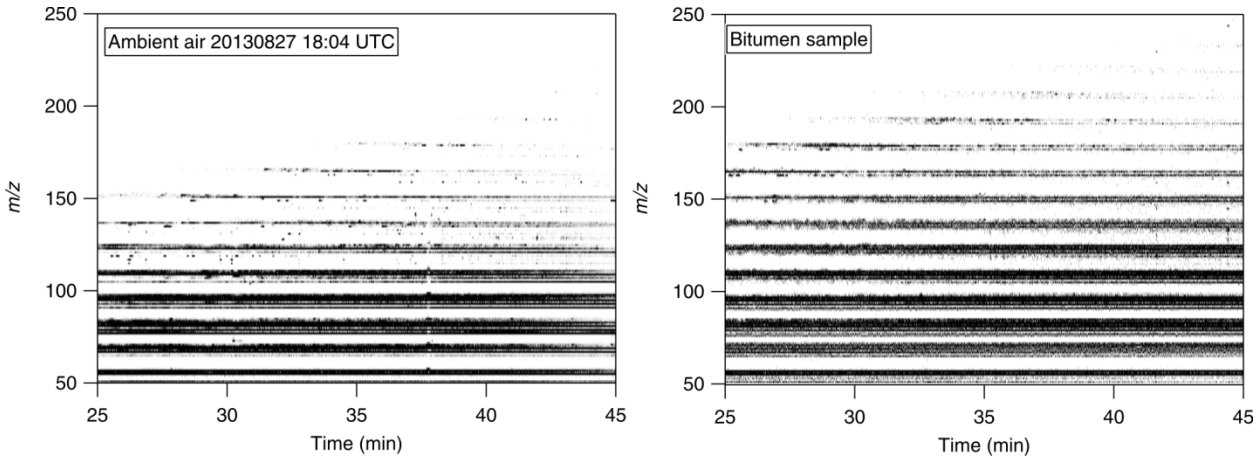

Figure S-1. Scatter of ions as a function of retention time for the total ion chromatograms shown in Figure 2 of the main manuscript. Darker pixels represent a higher intensity than lighter pixels.

Mixing ratios of carbon monoxide (CO), carbon dioxide (CO_2) and methane (CH_4) in ambient air were quantified using a commercial cavity ring-down spectrometer (Picarro G2401) (Nara et al., 2012; Chen et al., 2013). Ambient air was sampled from a height of 10 m through 0.635 cm outer diameter (o.d.) perfluoroalkoxyalkane (PFA) Teflon™ tubing and a 47 mm diameter, 1 µm pore filter at a flow rate of ~0.5 L min^{-1}. A scrubber ($MgClO_4$) was installed at the base of the sample line to remove water from the air. Operating procedures developed for Canada's greenhouse gas network of monitors across all stations in Canada by the Climate Division of ECCC were followed (ECCC, 2013a).The cavity ring-down spectrometer was calibrated every few days with calibrated standard gas mixtures (Scott-Marrin); a

target background mixture (CO_2 at a mixing ratio of 379.5 parts-per-million by volume (ppmv), CH_4 at 1.976 ppmv and CO at 198.4 parts-per-billion by volume (ppbv)) and a working mixture (CO_2 = 452.15 ppmv, CH_4 = 2.988 ppmv, CO = 494.5 ppbv). The estimated precision of 1 min data was $\pm$0.12 ppmv, $\pm$0.6 ppbv, and $\pm$1.89 ppbv for CO_2, CH_4 and CO respectively, while the estimated accuracy was < 1 ppmv, < 3 ppbv, and < 4 ppbv, respectively.

Mixing ratios of total odd nitrogen ($NO_y \equiv NO + NO_2 + \Sigma PAN + \Sigma AN + HNO_3 + HONO + 2N_2O_5 + ClNO_2 + ...$) were measured by a chemiluminescence analyzer equipped with a heated Molybdenum converter (Thermo 42i) as described elsewhere (Tokarek et al., 2014; Odame-Ankrah, 2015).

The total sulfur (TS) measurements were conducted using a thermal oxidizer (Thermo Scientific Model CON101) to convert TS to SO_2 and detected using a pulsed-fluorescence analyzer (Thermo Scientific, Model 43iTLE). SO_2 was measured directly with a second analyzer (Thermo Scientific, Model 43iTLE). Total reduced sulfur (TRS) mixing ratios were calculated by subtracting mixing ratios of SO_2 from TS.

Concentrations of particle-surface bound polycyclic aromatic hydrocarbons (pPAH) were measured using a photoelectric aerosol sensor (EcoChem Analytics, Model PAS 2000CE) (Wilson et al., 1994; Burtscher et al., 1982).

Two soot-particle aerosol mass spectrometers (SP-AMS, Aerodyne Research, Inc.) (Onasch et al., 2012) measured non-refractory PM_1 components. Both SP-AMS were high resolution time-of-flight aerosol mass spectrometers (HR-ToF-AMS) fitted with a diode pumped Nd:YAG 1064 nm laser vaporizer; one SP-AMS had its oven removed to measure black carbon containing particles only using the laser. Direct calibrations of rBC using mono-disperse "Regal Black" (Cabot Corp. R400) particles were carried out three times during the 2013 JOSM intensive study. Positive Matrix Factorization (PMF) was performed to identify the potential sources of organic aerosol as described in the companion study (Adam et al., in prep). Factors associated with primary aerosol, i.e., hydrocarbon-like organic aerosol (HOA), a less

oxidized oxygenated organic aerosol factor (LO-OOA) and measured refractory black carbon (rBC) were added as variables for PCA analysis. Mass spectra associated with LO-OOA exhibited H/C, O/C and N/C ratios of ~1.62, ~0.36, and ~0.004, respectively; while the O/C and N/C ratios are similar to HOA, the H/C ratio of LO-OOA more resembles the more oxidized OOA factor (MO-OOA) (Adam et al., in prep.).

Particle volumes were calculated (assuming spherical particle shapes) from sub- and super-micron size distributions acquired using a scanning mobility particle sizer (SMPS, TSI with a differential mobility analyzer model 3081 and condensation particle counter model 3776; PM_1) and a 0.071 cm impactor over the size range of 13.6 nm to 736.5 nm and an Aerodynamic Particle Sizer (APS, TSI 3321; PM_{10-1}) over the size range 1.04 µm to 10.4 µm, respectively. Both instruments were operated at ambient relative humidity. The SMPS sampled through conductive silicon tubing to minimize wall losses due to wall charges. The APS was operated from a container located on top of the trailer and sampled from a 1.6 m tall, ½ o.d. aluminum tube whose tip was bent into a U-shape.

An ambient ion monitor – ion chromatograph (AIM-IC) (Markovic et al., 2012) was used to measure hourly averaged gas-phase NH_3 and $PM_{2.5}$ particle-phase (i.e., of particles < 2.5 µm diameter) NH_4^+ concentrations. High time-resolution particle-phase NH_4^+ measurements made by the SP-AMS were scaled by interpolated phase ratios observed by AIM-IC to calculate gas-phase NH_3 concentrations at high time resolution. This approach assumes the same phase ratios for $PM_{2.5}$ as for PM_1.

Determination of optimum PCA solution

The full component pattern (before component removal, with rotation, i.e., showing 22 components for 22 variables) obtained for this data set is shown in Table S-2. A common challenge in PCA is the determination of the maximum number of components to retain in the analysis. Several criteria are used for this purpose: the latent root criterion, where only components with eigenvalues greater than 1 are considered significant, the 5% variance criterion, where the last component selected accounts for only a small portion (<5%) of the variance, the 95% cumulative percentage of variance criterion, where the extracted components account for at least 95% of the total variance, and the Scree test. In the latter, the eigenvalues are plotted against the number of components in the order of extraction (Fig. S-2); to avoid including too many components with unique variance, the number of acceptable components is located at the point where this plot becomes horizontal. The latent root criterion is most commonly used, but tends to extract too few components when the number of variables is < 20 (Hair et al., 1998). The Scree test, on the other hand, often requires "some art in administering it" (Cattell, 1966), i.e., is subjective, though generally results in the inclusion of two or three more components than the latent root criterion (Hair et al., 1998).

The maximum component number for each criterion are summarized in Table S-11. The Scree test plot (Fig. S-1) shows two plateaus where the slope becomes approximately horizontal: The first is located at N = 5 and the second at N = 12. The latent root criterion and the <5% variance method suggests a 7-component solution, whereas the >95% percentage of variance criterion suggests using a 10-component solution. Hair et al. (1998) recommend to examine component solutions with differing numbers of components to evaluate which best represents the structure of the variables. In the following, solutions are presented in ascending order of extracted components.

5-component solution

As a first attempt at interpretation of the PCA, the first cut-off of the Scree test criterion was chosen (N = 5 variables). The results (after Varimax rotation) are presented in Table S-3.

The 5-component solution accounts for a cumulative variance of 81.0 % after rotation. Communalities for the analysis, i.e., the fraction of total pollutant observations accounted for by the PCA (Otto, 2007), are greater than 70% for 18 variables. The lowest communalities were obtained for gas-phase ammonia (0.40), CO (0.48) and PM_{10-1} (0.51). TRS and the IVOCs were also relatively poorly represented (0.63 and 0.73, respectively). All eigenvalues are greater than 1.

The component accounting for most of the variance of the data, component 1, is strongly associated with all of the anthropogenic VOCs (with correlations of $r > 0.8$) and TRS ($r = 0.76$), weakly associated with CH_4 ($r = 0.62$), HOA ($r = 0.44$), LO-OOA ($r = 0.59$), IVOCs ($r = 0.47$), and CO ($r = 0.53$), and poorly associated with NO_y and TS ($r = 0.25$ and $r = 0.28$, respectively). Component 1 is consistent with tailings ponds emissions with potentially small contributions from nearby facilities (interpreted from weak and poor correlations with rBC ($r = 0.33$) and NO_y ($r = 0.25$)), which would otherwise remain unexplained.

Component 2 is strongly associated with the combustion tracers NO_y ($r = 0.83$), rBC ($r = 0.89$) and pPAH ($r = 0.83$) and weakly associated with IVOCs ($r = 0.61$), gas-phase ammonia ($r = 0.34$), undecane ($r = 0.31$), and CH_4 (0.38), but poorly and not with CO or CO_2 ($r = 0.19$ and 0.06, respectively); this component is identified as mine fleet emissions. Component 3 is strongly associated ($r > 0.9$) with the biogenic VOCs and weakly ($r = 0.55$) associated with CO_2 and is identified as a biogenic component.

Component 4 is strongly associated with SO_2 and TS ($r = 0.93$ and 0.91, respectively) and is consistent with emissions from upgrader facilities. These four components persisted, with little variation, in all solutions with a greater number of selected components (see below).

Component 5 is strongly associated with CO_2 ($r = 0.71$), and weakly associated with PM_{10-1} ($r = 0.57$), CH_4 ($r = 0.53$) and CO ($r = 0.40$). We are not aware of a source type that would fit this profile, i.e., combine

this particular set of pollutants without also being associated with NO_y (r = 0.02). This suggests that this component is an artifact arising from an insufficient number of components used in the analysis and motivates the inclusion of more components.

6-component solution

A 6-component solution is shown in Table S-4. Satisfying the percentage of variance criterion of the last component accounting for less than 5% of the variance (4.6% in this case, Table S-2) was selected. This solution accounts for a total variance of 85.23%. The first four components are essentially unchanged from the 5-component solution (with the exception of LO-OOA in component 2 becoming more poorly correlated (r = 0.22)). Component 5 is strongly associated with IVOCs (r = 0.70) and weakly associated with LO-OOA (r = 0.60), and TRS (r = 0.56). Component 6 is strongly associated with PM_{10-1} (r = 0.81) and weakly associated with CO_2 (r = 0.62), CH_4 (r = 0.41), HOA (r = 0.30) and NH_3 (r = 0.36) and, unlike the 5-component solution, not associated with CO.

7-component solution

Next, the latent root criterion gives a 7-component solution. The PCA results (after Varimax rotation) are presented in Table S-5. The seven components account for a cumulative variance of 88.7% after rotation. Communalities for the analysis are all greater than 60%, with the lowest communality obtained for CO (0.61). All eigenvalues are greater than 1.

Components 1 through 4 have the same associations with similar r values as those in the 5-component analysis, with the only significant exception a poorer association (r = 0.20) of component 2 with gas-phase ammonia.

The identifications of components 5 through 7 of the 7-component solution are murky at best. Component 5 is weakly associated with TRS (r = 0.56) and IVOCs (r = 0.66). Component 6 is strongly

208 associated with PM_{10-1} volume (r = 0.89), and weakly with CO_2 (r = 0.54), and CH_4 (r = 0.36) and appears
209 to be combination of a dust component with a source of greenhouse gases, whereas component 7 is
210 strongly associated with gas-phase ammonia (r = 0.82) and poorly associated with CO (r = 0.29). Both
211 appear to be amalgamations of distinct sources and suggest that too few components were selected.
212 Hair et al. (1998) note that the latent root criterion has a tendency to extract a conservative number of
213 components if the number of variables is < 20, close to the 22 variables in this analysis, consistent with
214 what is observed here. Hence, the 7-component solution is sub-optimal.
215
216 **8-component solution**
217 An 8-component solution is presented in Table S-6. Not satisfying any criterion, it is included here for
218 the sake of completeness. Owing to the inclusion of an additional component, the cumulative variance
219 improved to 91.6%. The greatest improvement was seen for CO, gas-phase ammonia, as well as the
220 IVOCs, whose communalities increased from 0.61, 0.91, and 0.80 (for the 7-component solution) to 0.96,
221 0.96 and 0.84, respectively.
222 The main effect of the inclusion of an additional component was the separation of component 7 into
223 two distinct components: one of these was strongly associated with gas-phase ammonia (r = 0.92), and
224 the other was strongly associated with CO (r = 0.85). A considerable fraction of the CO observed in the
225 region is generated as a byproduct of the photochemical oxidation of hydrocarbons (Shephard et al.,
226 2015); component 8 appears to capture this source, whereas component 1 captures the anthropogenic
227 emissions. The area near the oil sands mining operations is enriched in ammonia, which originates from
228 multiple sources: it is used as a floating agent to separate and recover bitumen from tar and is
229 generated during bitumen upgrading (called hydrotreating) in which N is removed as NH_3 and can be
230 present as a contaminant in tailing ponds. Other sources, such as agricultural activities, biological decay
231 processes, and smoldering fires are relatively minor in the region (Bytnerowicz et al., 2010). The poor

association of component 2 with ammonia (r = 0.22) may capture the use of ammonia as a floating agent, whereas component 8 embodies the remaining sources.

Component 5 is strongly associated with IVOCs (r = 0.71), and weakly associated with LO-OOA (r = 0.65) and TRS (r = 0.40). It is unclear if these variables originate from the same source or are forced together as a result of having chosen too few components. Considering that component 7 is split when an additional component is used (see below), the latter is more likely. Component 6 remains strongly associated with PM_{10-1} volume (r = 0.89), and weakly associated with CO_2 (r = 0.53), and CH_4 (r = 0.35) and is difficult to interpret. Because of the unclear classification of components 5 through 8, the 8-component solution is rejected.

9-component solution

A 9-component solution is presented in Table S-7. Components 1 through 8 describe sources that are qualitatively similar to those provided by the 8-component solution. Component 9 is strongly associated with TRS (r = 0.71) and poorly associated with o-xylene (r = 0.30); its profile is consistent with tailings ponds emission, where the presence of naphtha as a diluent gives rise to BTEX emissions and bacteria produce reduced sulfur compounds (Small et al., 2015; Warren et al., 2016). Component 6 is strongly associated with PM_{10-1} (r = 0.89) and weakly associated with CO_2 (r = 0.54) and CH_4 (r = 0.41). We have decided to reject this solution on the basis that < 95 % cumulative variance is observed.

10-component solution

Next, a 10-component solution with cumulative variance of 95.5%, satisfying the 95% criterion, was considered. With this solution, all communalities are >0.85 (Table 3). Component 6 is strongly associated with CO_2 (r = 0.77) and weakly associated with CH_4 (r = 0.59) but is not associated with other combustion tracers and is identified as inactive open-pit mines (see main text). Component 7 is strongly correlated

with PM_{10-1} (r = 0.93) and is identified as wind-blown dust. Component 8 and 9 are strongly associated with a single variable each, gas-phase ammonia (r = 0.94) and CO (r = 0.87), respectively. Component 10 is strongly associated with TRS (r = 0.71) and weakly associated with o-xylene (r = 0.32). Overall, this component is most consistent with a tailings ponds source, where the presence of naphtha as diluent gives rise to BTEX emissions, and sulfur-reducing bacteria are at work (Small et al., 2015; Warren et al., 2016). Overall, the 10-component solution was judged to be optimal.

11-component solution

The 11-component analysis is presented in Table S-8. Component 10 is now strongly associated with LO-OOA (r = 0.72) and weakly with rBC (r = 0.34) and has a low eigenvalue of 0.87. This solution is therefore rejected as we believe it contains too many components.

PCA without aerosol variables

A sensitivity test was conducted by which all aerosol species were removed as variables. The results of this sensitivity test are shown in Table S-10 and are presented as a 9-component solution, since the dust component associated with PM_{10-1} (component 7 in Table 5) cannot be generated when its main variable is removed.

The pattern in Table S-10 resembles that in Table 5 of the main manuscript, in that the same nine components emerged in both solutions with similar magnitude r values for each of the variables, including the IVOC signature. The only difference is that components 2 and 3 as well as 5 and 6 have traded places (i.e., the relative magnitudes of their eigenvalues, which were similar in Table 5, have switched), which is inconsequential. Furthermore, the correlation coefficients in Table S-10 are of similar magnitude (i.e., within $\pm$0.1) as those in Table 5, which suggests that IVOC to SOA conversion does not adversely affect the PCA, likely because of the proximity of the receptor site to sources.

Discussion of low-eigenvalue components

Component 6: A non-combustion source of CO_2 and CH_4

Component 6 of the analysis has a strong association with the greenhouse gases CO_2 ($r = 0.77$) and a weak association with CH_4 ($r = 0.59$) but is not associated with tracers of combustion (i.e., NO_y, pPAH, rBC) or naphtha (i.e., anthropogenic VOCs).

A significant amount of carbon is stored in bitumen, which, on geological time scales, conduces formation of CO_2 and CH_4 (i.e., natural gas) reservoirs and pools. When bitumen is mined, substantial emissions of CO_2 and, in particular, of CH_4 occur (Johnson et al., 2016). It is unclear, though, to what extent these greenhouse gases are released from "hot spots" (i.e., from a small number of locations) through surface cracks and fissures in the mine faces, or from new material that is exposed and then releases greenhouse gases during material handling, transport and processing (Johnson et al., 2016). The PCA analysis presented here would be more consistent with the "hot spots" hypothesis since component 6 is not associated with NOy, PAHs, or CO, which are expected to be emitted by the Diesel machinery involved in surface mining (i.e., active disturbance of the bitumen).

Another potential source contribution to component 6 is the degradation of peat and surface soil. Peatland soils, as they occur in the boreal forest surrounding the AMS 13 site, have long been recognized as important contributors to greenhouse gas fluxes and may also be contributing to component 6 (Miller et al., 2014; Gorham, 1991; Warner et al., 2017). The fixation and/or release of CO_2 as well as consumption and/or production of CH_4 through root, anaerobic and aerobic microbial respiration are dependent on soil conditions such as water table position, temperature, soil pH, and plant community composition (Yavitt et al., 2005; Oertel et al., 2016; Whalen, 2005). Emissions from peat and surface soil that was stripped as part of surface mining is expected to release between

303 1.1×10^{10} and 4.7×10^{10} kg stored carbon (Rooney et al., 2012), though it is unclear on what time scale this
304 release will occur. Some of this historical peat material is used for land reclamation. However, a
305 preliminary assessment of greenhouse gas fluxes from such a site gave no indication of significant
306 emissions, at least in the short term (Nwaishi et al., 2016). The bivariate polar plot shows that
307 component 6 is associated with no particular wind direction but with relatively low wind speeds (<
308 1.5 m/s; Figure S-7C), consistent with a dispersed surface source. Further, when variables associated
309 with secondary processes were added to the analysis (Table 7), component 6 anticorrelates with O_x
310 ($r = -0.41$). Dry deposition is a significant O_3 and NO_2, and therefore O_x, loss process (Wesely and Hicks,
311 2000; Zhang et al., 2002).

312 Overall, we have too little information to constrain soil fluxes for this data set. Considering the large CH_4
313 and CO_2 concentrations observed in this study, it is more likely that anthropogenic sources dominate
314 over natural soil emissions (Thompson et al., 2017). Future field campaigns at AMS 13 would benefit
315 from N_2O measurements to constrain contributions of natural sources to greenhouse gas
316 concentrations, such as those produced by microbes in water-logged soil.

317

318 **Component 7: Wind-blown dust**

319 Component 7 is correlated with PM_{10-1} ($r = 0.93$) and poorly with CO_2 ($r = 0.25$), HOA ($r = 0.23$), and LO-
320 OOA ($r = 0.25$). In the Athabasca oil sands region, surface mining has created large portions of land
321 whose surface is void of vegetation and is covered by sand and soil particles, which are readily
322 suspended by wind and vehicle traffic. Other mining activities add to the PM_{10-1} emissions, including
323 combustion processes, tailings sands, and mine haul roads, though the contributions of each of these to
324 the overall PM_{10-1} burden is uncertain (Wang et al., 2015). Recently, Phillips-Smith et al. investigated
325 metal species found in $PM_{2.5}$ aerosol at AMS 13 and found haul road dust and soil from mine faces to be

important sources of $PM_{2.5}$ (Phillips-Smith et al., 2017) and, likely, PM_{10-1} as well. The very poor associations of this component with CO_2 and CH_4 and lack of association with NO_y ($r = 0.02$) suggest contributions of open mine face soil in addition to dust suspended by vehicles travelling on unpaved roads.

The size range captured by PM_{10-1} may also include bioaerosol, including bacteria, fungal spores and plant pollen, which constitute the "natural" background aerosol over vegetated continental regions, typically contributing a few μg m^{-3} of aerosol mass (Huffman et al., 2010). Considering the large PM_{10-1} volumes observed in this work (Table 3), the contribution of bioaerosol is likely minor.

Component 8: Ammonia

Component 8 is a single variable component strongly associated with NH_3 ($r = 0.94$) but with no other variables.

Bytnerowicz et al. (2010) reported larger concentrations of NH_3 in the oil sands region than the provincial average. More recently, Shephard et al. (2015) reported enhancements of NH_3 in the general area as judged from satellite observations. Both studies hence suggest the existence of anthropogenic sources, though Shephard et al. (2015) speculated that biomass burning can contribute to the ammonia burden in the region. A recent modelling study by Whaley et al. (2018) estimated that around half of near-surface NH_3 during the study was likely from bi-directional exchange (i.e., re-emission from soil and plants).

In the oil sands, NH_3 is used as a floating agent for the separation and recovery of bitumen from tar, during bitumen upgrading in a process called "hydrotreating", and in tailing ponds, which, on occasion, have been contaminated with NH_3 to such a degree that they outgas it (Bytnerowicz et al., 2010).

Ammonia is also used for flue gas de-sulfurization by Syncrude; emission inventories (NPRI, 2013; ECCC, 2013b) suggest their fugitive emissions are the largest anthropogenic source in the region, though it is not clear if all sources are accurately inventoried.

The lack of association of ammonia with other variables in this component and the bivariate polar plots (Figure S-9) are consistent with an NH_3-specific source profile, such as fugitive emissions from one or more point sources that emit independently from other activities (i.e., ammonia storage tanks) and natural emissions from soil and trees (Whaley et al., 2018).

Component 9: Incomplete hydrocarbon oxidation

Component 9 is another single variable component and strongly correlates with CO (r = 0.87).The conventional interpretation of CO is as a byproduct of incomplete VOC oxidation, as it is found in fossil fuel combustion exhaust or in biomass burning plumes. Component 9, however, is not associated with NO_y (r = -0.08) or CO_2 (r = 0.05), which rules out this conventional interpretation.

Recently, Marey et al. (2015) examined the spatial distribution of CO in Northern Alberta using a combination of satellite and ground station data and found that most CO is derived from anthropogenic sources, biomass burning and the photochemical oxidation of methane and other VOCs. During the 2013 JOSM study, there was no obvious (i.e., tracer) evidence for fire emissions impacting the measurements at AMS 13 (Phillips-Smith et al., 2017), though an impact from distant sources (such as fires located 1,000s of km upwind in British Columbia or Washington State) cannot be entirely ruled out. We therefore interpret component 9 as a VOC oxidation product component.

Component 10: Dry tailings

Component 10 is strongly associated with TRS (r = 0.71) and weakly with o-xylene (r = 0.32) and poorly with IVOCs (r= 0.20). This component is qualitatively similar to component 1, in that the presence of o-xylene suggests emission of naphtha, and the presence of TRS suggests anaerobic sulfur reducing bacteria and methanogens as they occur in tailings ponds (Holowenko et al., 2000; Percy, 2013; Quagraine et al., 2005). However, the absence of correlations with NO_y, rBC, and CO suggests that this source is not in spatial proximity with a continuously operating combustion source. The much poorer correlations of o-xylene, CH_4, and IVOCs than for component 1 suggests that this component is much more "aged", i.e., emits less naphtha and bitumen.

As part of the reclamation process, tailings ponds in the Alberta oil sands region are converted into "composite tailings", which consist of a consolidated alkaline, saline mixture of processed sand, residual bitumen, clay fines, and gypsum ($CaSO_4$). This mixture settles and releases water, forming shallow pools of surface water (Figure 4J). Due to intensive microbial activity, composite tailings deposits are strong sources of H_2S and, likely, other reduced sulfur species (Warren et al., 2016; Bradford et al., 2017). Composite tailings are a source consistent with the emission profile of component 10. The association with TRS is explained by its production from biological activity and the presence of IVOCs by outgassing from the residual bitumen. Syncrude (the company operating closest to AMS 13) has been undertaking a pilot scale wetland reclamation project in the Athabasca Oil Sands Region to allow the development of a fen wetland above composite tailings (Bradford et al., 2017). Component 10 is hence interpreted as a dry tailings pond component, though the confidence in this interpretation is somewhat marginal as judged, for example, from the low eigenvalue of 0.74.

Bivariate polar plots

Bivariate polar plots map a surface using wind direction and wind speed and then model pollutant concentrations. While PCA is good at showing the temporal distribution of sources, bivariate polar plots help to show the spatial distribution of sources.

Figure S-3 shows a sample of variables associated with component 1. This component appears to dominate when winds are from the SSE and E and of moderate wind speeds (2-3 m/s).

Figure S-4 shows a sample of dominant variables associated with component 2. This component appears to dominate when winds are from the E at low wind speeds (1-2 m/s). The map appears to track the location of the Athabasca river and highway 63, corroborating that this source is from vehicular emissions.

Figure S-5 shows a sample of dominant variables associated with component 3. This component appears to dominate when winds are stagnant and local. This is unsurprising because biogenic emissions are expected to be emitted in great concentrations locally since our site is surrounded on all sides by forest.

Figure S-6 shows a sample of dominant variables associated with component 4 (or with component 2 in the secondary processes PCA). This component appears to dominate when winds are moderate (2-3 m/s) and from the SE and E.

Figure S-7 shows a sample of dominant variables associated with component 5. This component appears to dominate when winds are from the E at moderate wind speeds (2-3 m/s).

Figure S-8 shows a sample of dominant variables associated with component 6. This component appears to dominate when winds are stagnant and local. This suggests that this source is biogenic and may be due to emissions from trees.

Figure S-9 shows a sample of dominant variables associated with component 7. This component appears to dominate when winds are from the SE and E at moderate wind speeds (1-3 m/s).

Figure S-10 shows a sample of dominant variables associated with component 8. This component does

not appear to have a specific direction associated with it and is observed in all directions. This component is observed when winds are at moderate to high speeds (2-4 m/s).

Figure S-11 shows a sample of dominant variables associated with component 9. This component is observed when winds are from the S, SE, and E. This component is observed when winds are at low to moderate speeds (1-3 m/s).

Figure S-12 shows a sample of dominant variables associated with component 10. This component is observed when winds are from the SSE. This component is observed when winds are around 1.5 m/s. This source is very likely a point source due to its consistency with wind direction and speed.

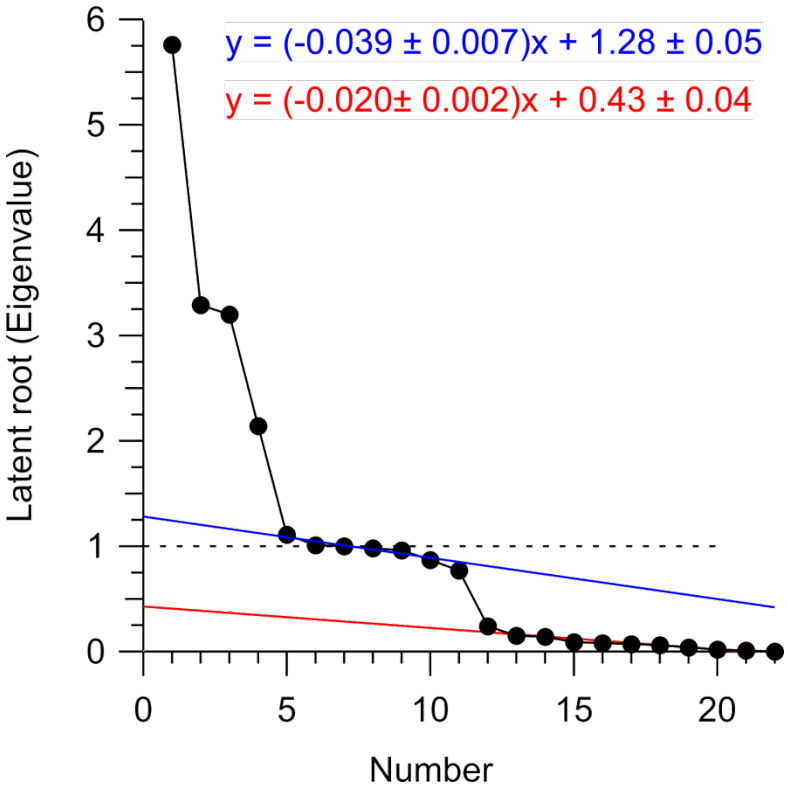

Figure S-2. Scree plot used to consider the number of components to retain. Dashed line represents the latent root criterions (eigenvalues > 1). Blue line represents the first instance of eigenvalues becoming

426 horizontal. Red line represents the second instance of eigenvalues becoming horizontal.

427

428 **Table S-1.** Ionimed Analytical GCU Standard.

Compound	Volume mixing ratio (ppmv)	Uncertainty (%)
Formaldehyde	1.01	±8
Methanol	1.01	±8
Acetonitrile	1.01	±6
Acetaldehyde	1.01	±5
Ethanol	1.01	±8
Acrolein	0.98	±5
Acetone	1.02	±5
Isoprene	0.99	±5
Crotonaldehyde	0.92	±6
2-Butanone	1.01	±5
Benzene	1.01	±5
Toluene	1.02	±5
o-xylene	1.03	±6
Chlorobenzene	1.02	±5
α-pinene	0.93	±5
1,2, Dichlorobenzene	1.03	±7
1,2,4-Trichlorobenzene	1.01	±9

429

Table S-2. The component pattern after Varimax rotation. Correlations greater than 0.30 or less than -0.30 are bolded.

	1	2	3	4	5	6	7	8	9	10	11	12	13	14	15	16	17	18	19	20	21	22
Anthropogenic VOCs																						
o-xylene	**0.89**	0.07	0.03	0.10	0.09	0.06	-0.03	0.11	0.15	0.06	0.26	0.11	0.00	0.04	-0.08	0.24	0.00	-0.01	-0.02	0.00	-0.01	0.00
1,2,3 - TMB	**0.94**	0.15	0.07	0.06	0.05	0.08	-0.01	0.06	0.17	0.01	-0.01	0.02	-0.04	0.01	-0.08	-0.14	0.03	0.00	-0.09	0.00	-0.07	0.00
1,2,4 - TMB	**0.94**	0.13	0.01	0.11	0.08	0.05	-0.02	0.09	0.17	0.04	0.12	0.03	-0.01	0.02	-0.06	0.03	0.01	0.00	-0.04	0.00	0.09	0.00
decane	**0.91**	0.22	-0.02	0.15	0.05	0.00	0.04	0.15	0.05	0.15	0.07	-0.02	0.04	-0.01	0.07	-0.03	-0.03	0.02	0.16	0.00	-0.01	0.00
undecane	**0.85**	0.27	-0.08	0.23	0.08	-0.03	0.06	0.05	0.00	0.20	0.01	-0.10	0.09	0.00	0.26	-0.05	-0.02	0.02	0.02	0.00	0.00	0.00
Biogenic VOCs																						
α-pinene	-0.03	-0.08	**0.98**	-0.11	0.02	0.05	-0.08	0.02	0.01	0.00	-0.01	0.02	0.00	0.00	-0.01	0.01	-0.08	-0.01	0.00	0.09	0.00	0.00
ß-pinene	-0.02	-0.08	**0.97**	-0.12	0.01	0.05	-0.08	0.01	0.01	0.01	0.01	-0.02	0.00	-0.02	0.02	0.00	-0.10	0.01	0.01	-0.09	0.00	0.00
limonene	0.08	-0.02	**0.92**	-0.08	0.06	0.23	-0.11	0.08	0.02	0.07	-0.05	0.02	-0.03	0.03	-0.02	0.00	0.23	0.00	-0.01	0.00	0.00	0.00
Combustion tracers																						
NO_y	0.26	**0.80**	-0.25	0.21	0.03	-0.05	0.10	0.19	-0.04	0.07	0.04	0.01	**0.34**	0.00	0.04	0.00	-0.01	-0.01	0.01	0.00	0.00	0.00
rBC	**0.31**	**0.80**	0.03	0.05	0.08	0.07	0.11	0.24	0.12	**0.34**	-0.03	0.02	-0.02	-0.05	0.02	-0.01	0.00	0.22	0.01	0.00	0.00	0.00
CO	**0.41**	0.18	0.04	0.02	0.08	0.07	0.05	0.03	**0.88**	0.06	0.00	0.02	0.00	0.01	0.00	0.00	0.00	0.00	0.00	0.00	0.00	0.00
CO_2	0.10	0.09	**0.46**	-0.12	0.23	**0.82**	-0.14	-0.03	0.07	0.00	-0.05	0.02	-0.01	0.01	0.00	0.00	0.00	0.00	0.00	0.00	0.00	0.00
Aerosol species																						
pPAH	0.07	**0.94**	-0.08	-0.11	0.02	0.06	0.14	0.00	0.09	-0.15	0.00	0.01	-0.14	-0.07	-0.02	0.00	0.00	-0.10	0.00	0.00	0.00	0.00
PM_{10-1}	0.18	0.13	0.07	0.10	**0.94**	0.16	-0.03	0.04	0.07	0.10	0.08	0.02	0.00	0.01	0.00	0.00	0.00	0.00	0.00	0.00	0.00	0.00
HOA	**0.41**	**0.74**	0.02	0.11	0.21	0.11	-0.04	0.13	0.15	0.19	0.10	0.05	0.01	**0.35**	0.00	0.01	0.01	-0.01	0.00	0.00	0.00	0.00
LO-OOA	**0.45**	0.17	0.13	0.25	0.19	0.01	-0.04	0.28	0.10	0.73	0.16	0.02	0.01	0.03	0.01	0.00	0.00	0.00	0.00	0.00	0.00	0.00
Sulfur																						
TS	0.25	0.04	-0.16	**0.94**	0.07	-0.05	-0.02	0.02	0.01	0.09	0.14	0.00	0.01	0.01	0.01	0.00	0.00	0.00	0.00	0.00	0.00	0.01
SO_2	0.11	0.02	-0.15	**0.98**	0.04	-0.04	-0.03	-0.02	0.01	0.05	-0.05	-0.01	0.01	0.01	0.00	0.00	0.00	0.00	0.00	0.00	0.00	-0.01
TRS	**0.57**	0.05	-0.08	0.11	0.14	-0.05	0.03	0.16	-0.01	0.13	**0.77**	0.02	0.00	0.01	0.00	0.00	0.00	0.00	0.00	0.00	0.00	0.00
Other																						
IVOCs	**0.34**	**0.34**	0.12	-0.03	0.05	-0.02	-0.02	**0.84**	0.04	0.18	0.13	0.01	0.01	0.01	0.00	0.00	0.00	0.00	0.00	0.00	0.00	0.00
NH_3	0.01	0.19	-0.23	-0.04	-0.03	-0.09	**0.95**	-0.01	0.04	-0.01	0.01	0.00	0.01	0.00	0.00	0.00	0.00	0.00	0.00	0.00	0.00	0.00
CH_4	**0.60**	**0.39**	0.10	-0.05	0.14	0.44	0.00	0.06	0.16	0.08	0.09	**0.46**	0.01	0.03	-0.02	0.01	0.00	0.00	0.00	0.00	0.00	0.00
Eigenvalues	5.76	3.29	3.20	2.14	1.11	1.01	1.00	0.98	0.96	0.87	0.77	0.24	0.15	0.14	0.09	0.08	0.07	0.06	0.04	0.02	0.01	0.00
% of variance	26.17	14.97	14.55	9.75	5.06	4.60	4.53	4.46	4.34	3.94	3.51	1.09	0.69	0.63	0.42	0.37	0.33	0.28	0.17	0.08	0.06	0.00
% cum. var.	26.17	41.14	55.69	65.43	70.49	75.09	79.62	84.07	88.42	92.36	95.87	96.97	97.66	98.29	98.71	99.08	99.41	99.69	99.86	99.94	100.0	100

Table S-3. The pattern after Varimax rotation with 5 components selected.

	1	2	3	4	5	Communalities
Anthropogenic VOCs						
o-xylene	**0.94**	0.08	0.03	0.09	0.15	0.93
1,2,3 - TMB	**0.90**	0.14	0.04	0.01	0.23	0.89
1,2,4 - TMB	**0.95**	0.14	-0.01	0.09	0.18	0.97
decane	**0.91**	0.27	-0.03	0.16	0.05	0.93
undecane	**0.82**	**0.31**	-0.10	0.26	0.05	0.84
Biogenic VOCs						
α-pinene	-0.03	-0.05	**0.94**	-0.15	0.04	0.91
ß-pinene	-0.02	-0.06	**0.94**	-0.15	0.03	0.90
limonene	0.07	0.02	**0.94**	-0.10	0.18	0.93
Combustion tracers						
NO_y	0.25	**0.83**	-0.29	0.22	0.02	0.89
rBC	**0.33**	**0.89**	0.04	0.07	0.13	0.92
CO	**0.53**	0.19	-0.02	-0.08	**0.40**	0.48
CO_2	0.07	0.06	**0.55**	-0.13	**0.71**	0.83
Aerosol species						
pPAH	0.01	**0.83**	-0.20	-0.20	0.27	0.84
PM_{10-1}	0.21	0.19	0.15	0.29	**0.57**	0.51
HOA	**0.44**	**0.75**	0.03	0.15	**0.32**	0.88
LO-OOA	**0.59**	**0.37**	0.28	0.41	-0.06	0.74
Sulfur						
TS	0.28	0.04	-0.18	**0.91**	0.01	0.94
SO_2	0.10	0.01	-0.18	**0.93**	0.05	0.91
TRS	**0.76**	0.10	-0.04	0.17	-0.13	0.63
Other						
IVOCs	**0.47**	**0.61**	0.28	0.03	-0.25	0.73
NH_3	0.02	**0.34**	**-0.47**	-0.21	-0.14	0.40
CH_4	**0.62**	**0.38**	0.12	-0.09	**0.53**	0.84
Eigenvalues	6.42	3.79	3.56	2.34	1.70	
% of variance	29.20	17.25	16.20	10.63	7.74	
Cumulative variance	29.20	46.45	62.65	73.28	81.01	

Table S-4. The pattern after Varimax rotation with 6 components selected.

	1	2	3	4	5	6	Communalities
Anthropogenic VOCs							
o-xylene	**0.92**	0.04	0.01	0.08	0.24	0.13	0.93
1,2,3 - TMB	**0.94**	0.16	0.08	0.07	0.06	0.05	0.92
1,2,4 - TMB	**0.95**	0.13	0.00	0.11	0.16	0.08	0.97
decane	**0.88**	0.23	-0.02	0.18	0.28	0.00	0.94
undecane	**0.79**	0.28	-0.09	0.29	0.25	0.00	0.85
Biogenic VOCs							
α-pinene	-0.02	-0.09	**0.96**	-0.12	0.04	0.01	0.95
ß-pinene	-0.02	-0.10	**0.96**	-0.12	0.05	0.01	0.94
limonene	0.09	-0.01	**0.95**	-0.09	0.04	0.15	0.95
Combustion tracers							
NO_y	0.22	**0.81**	-0.27	0.23	0.25	0.00	0.89
rBC	**0.31**	**0.85**	0.07	0.08	0.28	0.10	0.92
CO	**0.64**	0.29	0.09	0.02	-0.23	0.09	0.56
CO_2	0.17	0.12	**0.57**	-0.17	-0.23	**0.62**	0.84
Aerosol species							
pPAH	0.09	**0.90**	-0.10	-0.14	-0.10	0.05	0.87
PM_{10-1}	0.19	0.14	0.03	0.12	0.17	**0.81**	0.76
HOA	**0.44**	**0.73**	0.04	0.13	0.22	**0.30**	0.88
LO-OOA	**0.46**	0.22	0.17	**0.32**	**0.60**	0.21	0.79
Sulfur							
TS	0.25	0.02	-0.18	**0.92**	0.12	0.06	0.97
SO_2	0.10	0.03	-0.15	**0.97**	-0.02	0.02	0.98
TRS	**0.62**	-0.04	-0.17	0.06	**0.56**	0.14	0.75
Other							
IVOCs	**0.31**	**0.43**	0.17	-0.06	**0.70**	0.02	0.80
NH_3	0.06	**0.41**	**-0.36**	-0.11	-0.11	**-0.36**	0.46
CH_4	**0.68**	**0.42**	0.15	-0.10	0.00	**0.41**	0.84
Eigenvalues	6.09	3.60	3.47	2.25	1.76	1.58	
% of variance	27.70	16.38	15.78	10.22	7.98	7.18	
Cumulative variance	27.70	44.07	59.85	70.08	78.06	85.23	

Table S-5. The pattern after Varimax rotation with 7 components selected.

	1	2	3	4	5	6	7	Commu-nalities
Anthropogenic VOCs								
o-xylene	**0.93**	0.07	0.01	0.08	0.21	0.12	-0.05	0.93
1,2,3 - TMB	**0.94**	0.18	0.08	0.06	0.03	0.03	-0.03	0.93
1,2,4 - TMB	**0.96**	0.15	0.00	0.11	0.14	0.07	-0.02	0.98
decane	**0.88**	0.26	-0.02	0.18	0.26	0.00	0.01	0.94
undecane	**0.79**	**0.30**	-0.09	0.28	0.23	0.00	0.03	0.85
Biogenic VOCs								
α-pinene	-0.03	-0.09	**0.96**	-0.11	0.04	0.00	-0.05	0.96
ß-pinene	-0.02	-0.10	**0.96**	-0.11	0.06	0.01	-0.05	0.95
limonene	0.09	0.01	**0.95**	-0.08	0.03	0.12	-0.13	0.95
Combustion tracers								
NO_y	0.22	**0.83**	-0.28	0.22	0.20	-0.02	0.06	0.91
rBC	**0.31**	**0.85**	0.07	0.08	0.25	0.11	0.13	0.92
CO	**0.62**	0.22	0.13	0.03	-0.21	0.19	0.29	0.61
CO_2	0.17	0.17	**0.56**	-0.18	-0.28	**0.54**	-0.27	0.84
Aerosol species								
pPAH	0.08	**0.89**	-0.10	-0.15	-0.14	0.03	0.15	0.88
PM_{10-1}	0.18	0.12	0.06	0.13	0.18	**0.89**	0.01	0.89
HOA	**0.44**	**0.76**	0.03	0.12	0.16	0.27	-0.03	0.89
LO-OOA	**0.46**	0.23	0.18	**0.33**	**0.59**	0.25	0.01	0.81
Sulfur								
TS	0.25	0.04	-0.18	**0.92**	0.12	0.06	-0.02	0.97
SO_2	0.10	0.04	-0.15	**0.97**	-0.02	0.02	-0.03	0.98
TRS	**0.62**	-0.03	-0.16	0.07	**0.56**	0.19	0.02	0.77
Other								
IVOCs	**0.32**	**0.48**	0.16	-0.07	**0.66**	0.00	-0.05	0.80
NH_3	0.01	0.20	-0.26	-0.06	0.00	-0.05	**0.89**	0.91
CH_4	**0.68**	**0.45**	0.15	-0.11	-0.05	**0.36**	-0.10	0.85
Eigenvalues	6.09	3.65	3.42	2.23	1.61	1.46	1.03	
% of variance	27.70	16.60	15.57	10.14	7.33	6.66	4.70	
Cumulative variance	27.70	44.30	59.86	70.01	77.34	84.00	88.70	

Table S-6. The pattern after Varimax rotation with 8 components selected.

	1	2	3	4	5	6	7	8	Communalities
Anthropogenic VOCs									
o-xylene	**0.93**	0.08	0.03	0.07	0.14	0.13	-0.03	0.11	0.93
1,2,3 - TMB	**0.91**	0.19	0.09	0.06	-0.01	0.02	-0.04	0.21	0.93
1,2,4 - TMB	**0.95**	0.16	0.01	0.11	0.09	0.07	-0.03	0.18	0.98
decane	**0.90**	0.26	-0.01	0.17	0.19	0.01	0.03	0.08	0.95
undecane	**0.82**	**0.30**	-0.07	0.28	0.15	0.01	0.06	0.03	0.87
Biogenic VOCs									
α-pinene	-0.04	-0.10	**0.97**	-0.11	0.06	0.00	-0.05	0.00	0.96
ß-pinene	-0.02	-0.10	**0.96**	-0.11	0.06	0.00	-0.04	-0.01	0.96
limonene	0.07	0.00	**0.95**	-0.08	0.06	0.11	-0.14	0.05	0.95
Combustion tracers									
NO_y	0.25	**0.83**	-0.26	0.22	0.19	-0.01	0.10	-0.08	0.92
rBC	0.28	**0.83**	0.06	0.07	**0.33**	0.10	0.09	0.17	0.93
CO	**0.42**	0.18	0.04	0.01	0.07	0.11	0.06	**0.85**	0.96
CO_2	0.13	0.19	**0.58**	-0.17	-0.28	**0.53**	-0.27	0.10	0.86
Aerosol species									
pPAH	0.06	**0.91**	-0.08	-0.14	-0.11	0.03	0.16	0.06	0.89
PM_{10-1}	0.18	0.12	0.07	0.12	0.16	**0.89**	0.01	0.06	0.89
HOA	**0.42**	**0.75**	0.03	0.12	0.21	0.26	-0.06	0.15	0.89
LO-OOA	**0.46**	0.19	0.15	**0.30**	**0.65**	0.24	-0.04	0.15	0.87
Sulfur									
TS	0.28	0.03	-0.18	**0.92**	0.09	0.07	-0.01	-0.02	0.97
SO_2	0.11	0.04	-0.15	**0.97**	-0.01	0.02	-0.04	0.03	0.98
TRS	**0.72**	-0.03	-0.13	0.06	**0.40**	0.23	0.11	-0.20	0.80
Other									
IVOCs	**0.35**	**0.43**	0.13	-0.09	**0.71**	0.00	-0.07	0.01	0.84
NH_3	0.01	0.22	-0.24	-0.05	-0.05	-0.04	**0.92**	0.05	0.96
CH_4	**0.65**	**0.47**	0.17	-0.11	-0.08	**0.35**	-0.10	0.16	0.86
Eigenvalues	5.99	3.58	3.40	2.20	1.52	1.43	1.03	1.00	
% of variance	27.23	16.28	15.44	10.01	6.90	6.52	4.70	4.53	
Cumulative variance	27.23	43.51	58.95	68.96	75.86	82.37	87.08	91.61	

Table S-7. The pattern after Varimax rotation with 9 components selected.

	1	2	3	4	5	6	7	8	9	Communalities
Anthropogenic VOCs										
o-xylene	**0.89**	0.09	0.03	0.09	0.11	0.11	-0.05	0.16	**0.30**	0.95
1,2,3 - TMB	**0.93**	0.16	0.08	0.05	0.05	0.05	-0.02	0.17	-0.02	0.94
1,2,4 - TMB	**0.94**	0.15	0.01	0.11	0.11	0.08	-0.02	0.18	0.12	0.98
decane	**0.91**	0.22	-0.03	0.16	0.25	0.04	0.05	0.03	0.03	0.97
undecane	**0.85**	0.25	-0.10	0.25	0.24	0.06	0.10	-0.05	-0.08	0.94
Biogenic VOCs										
α-pinene	-0.04	-0.09	**0.97**	-0.10	0.05	0.00	-0.06	0.02	0.02	0.97
ß-pinene	-0.03	-0.10	**0.97**	-0.11	0.05	0.00	-0.05	0.00	0.02	0.96
limonene	0.09	-0.01	**0.94**	-0.09	0.08	0.13	-0.13	0.03	-0.06	0.95
Combustion tracers										
NO_y	0.26	**0.82**	-0.26	0.22	0.22	0.00	0.11	-0.09	0.02	0.92
rBC	**0.31**	**0.79**	0.04	0.05	**0.41**	0.12	0.12	0.12	-0.10	0.94
CO	**0.42**	0.19	0.05	0.02	0.08	0.10	0.06	**0.87**	-0.02	0.98
CO_2	0.16	0.17	**0.56**	-0.18	-0.22	**0.56**	-0.25	0.06	-0.17	0.86
Aerosol species										
pPAH	0.06	**0.93**	-0.07	-0.12	-0.11	0.01	0.14	0.09	0.03	0.93
PM_{10-1}	0.16	0.11	0.06	0.12	0.17	**0.89**	0.02	0.06	0.10	0.89
HOA	**0.41**	**0.75**	0.03	0.13	0.23	0.25	-0.06	0.16	0.08	0.90
LO-OOA	**0.46**	0.14	0.13	0.28	0.70	0.26	-0.01	0.10	0.05	0.90
Sulfur										
TS	0.25	0.04	-0.17	**0.93**	0.08	0.06	-0.02	0.00	0.13	0.99
SO_2	0.11	0.03	-0.15	**0.97**	0.01	0.02	-0.03	0.01	-0.05	0.99
TRS	**0.59**	0.05	-0.09	0.11	0.24	0.14	0.04	-0.04	**0.71**	0.96
Other										
IVOCs	**0.32**	**0.41**	0.12	-0.09	**0.70**	-0.01	-0.08	0.02	0.20	0.84
NH_3	0.01	0.21	-0.24	-0.05	-0.04	-0.04	**0.93**	0.04	0.01	0.97
CH_4	**0.65**	**0.47**	0.16	-0.10	-0.06	**0.36**	-0.10	0.17	0.07	0.86
Eigenvalues	5.84	3.44	3.37	2.19	1.58	1.47	1.03	0.95	0.74	
% of variance	26.54	15.63	15.30	9.98	7.19	6.66	4.69	4.31	3.38	
Cumulative variance	26.54	42.17	57.47	67.44	74.63	81.29	85.98	90.29	93.67	

441 **Table S-8.** The factor pattern after Varimax rotation with 11 factors selected.

	Factor 1	Factor 2	Factor 3	Factor 4	Factor 5	Factor 6	Factor 7	Factor 8	Factor 9	Factor 10	Factor 11	Commu-nalities
Anthropogenic VOCs												
o-xylene	**0.88**	0.08	0.03	0.10	0.13	0.07	-0.04	0.17	0.11	0.04	**0.32**	0.95
1,2,3 - TMB	**0.94**	0.16	0.07	0.05	0.11	0.05	-0.01	0.18	0.06	-0.01	-0.02	0.96
1,2,4 - TMB	**0.94**	0.15	0.01	0.11	0.08	0.08	-0.02	0.18	0.09	0.03	0.13	0.99
decane	**0.92**	0.24	-0.02	0.15	0.00	0.05	0.04	0.04	0.13	0.16	0.05	0.97
undecane	**0.87**	0.29	-0.08	0.22	-0.06	0.09	0.05	-0.05	0.03	0.22	-0.05	0.96
Biogenic VOCs												
α-pinene	-0.03	-0.08	**0.98**	-0.11	0.04	0.01	-0.08	0.02	0.02	0.00	0.00	0.98
ß-pinene	-0.02	-0.08	**0.98**	-0.12	0.02	0.02	-0.07	0.00	0.00	0.02	0.01	0.98
limonene	0.08	-0.02	**0.93**	-0.08	0.24	0.05	-0.11	0.03	0.09	0.06	-0.05	0.95
Combustion tracers												
NO_y	0.27	**0.83**	-0.26	0.21	-0.04	0.03	0.10	-0.08	0.18	0.07	0.01	0.92
rBC	**0.30**	**0.81**	0.04	0.04	0.09	0.07	0.12	0.12	0.23	**0.34**	-0.05	0.95
CO	**0.41**	0.19	0.04	0.02	0.08	0.08	0.05	**0.87**	0.03	0.06	-0.01	0.99
CO_2	0.09	0.08	**0.48**	-0.12	**0.77**	0.25	-0.14	0.05	-0.04	-0.01	-0.09	0.95
Aerosol species												
pPAH	0.06	**0.93**	-0.07	-0.12	0.07	0.02	0.14	0.10	-0.02	-0.20	0.01	0.95
PM_{10-1}	0.18	0.14	0.08	0.10	0.17	**0.94**	-0.03	0.07	0.04	0.09	0.08	1.00
HOA	**0.40**	**0.77**	0.03	0.11	0.14	0.20	-0.07	0.16	0.09	0.19	0.13	0.92
LO-OOA	**0.45**	0.19	0.13	0.25	0.03	0.19	-0.04	0.11	0.27	**0.72**	0.16	0.98
Sulfur												
TS	0.26	0.05	-0.16	**0.93**	-0.05	0.07	-0.02	0.01	0.02	0.08	0.13	0.26
SO_2	0.12	0.03	-0.15	**0.98**	-0.04	0.04	-0.03	0.01	-0.02	0.05	-0.05	0.12
TRS	**0.58**	0.06	-0.08	0.10	-0.04	0.14	0.03	-0.03	0.16	0.13	**0.74**	0.58
Other												
IVOCs	**0.34**	**0.37**	0.13	-0.03	-0.01	0.05	-0.03	0.03	**0.82**	0.18	0.12	1.00
NH_3	0.01	0.20	-0.24	-0.04	-0.08	-0.03	**0.94**	0.04	-0.02	-0.01	0.01	1.00
CH_4	**0.59**	**0.40**	0.10	-0.06	**0.59**	0.10	0.00	0.17	0.05	0.07	0.15	0.93
Eigenvalues	5.75	3.43	3.24	2.13	1.12	1.10	0.99	0.96	0.93	0.87	0.79	
% var.	26.14	15.61	14.72	9.66	5.11	4.99	4.51	4.35	4.22	3.95	3.60	
% Cum. var.	26.14	41.74	56.46	66.12	71.23	76.22	80.73	85.09	89.31	93.26	96.86	

Table S-9. The pattern with mixing height included after Varimax rotation with 10 components.

	1	2	3	4	5	6	7	8	9	10	Commu-nalities
Anthropogenic VOCs											
o-xylene	**0.89**	0.04	0.03	0.10	0.29	0.10	-0.01	-0.06	0.17	0.16	0.95
1,2,3 - TMB	**0.94**	0.17	0.10	0.04	-0.04	0.01	-0.03	-0.04	0.17	0.06	0.95
1,2,4 - TMB	**0.94**	0.13	0.03	0.10	0.11	0.09	-0.02	-0.06	0.18	0.07	0.98
decane	**0.92**	0.25	0.03	0.15	0.11	0.11	0.01	0.04	0.03	-0.04	0.97
undecane	**0.87**	**0.31**	-0.05	0.23	-0.03	0.17	0.03	0.10	-0.05	-0.11	0.96
Biogenic VOCs											
α-pinene	-0.02	-0.08	**0.96**	-0.10	0.03	0.01	-0.05	-0.11	0.01	0.02	0.96
ß-pinene	-0.01	-0.08	**0.96**	-0.11	0.04	0.02	-0.05	-0.12	-0.01	0.02	0.96
limonene	0.11	0.02	**0.95**	-0.08	0.04	0.02	-0.11	-0.06	0.03	0.12	0.96
Combustion tracers											
NO_y	0.21	**0.86**	-0.25	0.21	0.11	0.06	0.10	0.01	-0.08	-0.02	0.92
rBC	0.29	**0.89**	0.12	0.02	0.10	0.19	0.03	0.09	0.10	-0.01	0.95
CO	**0.43**	0.20	0.04	0.01	0.00	0.08	0.02	0.05	**0.86**	0.07	0.98
CO_2	0.15	0.17	**0.56**	-0.13	-0.12	0.13	-0.14	-0.12	0.08	**0.68**	0.91
Aerosol species											
pPAH	0.01	**0.86**	-0.09	-0.13	-0.08	-0.03	0.23	-0.18	0.12	0.17	0.90
PM_{10-1}	**0.31**	0.22	0.05	0.15	0.12	**0.88**	0.04	-0.01	0.08	0.10	0.97
HOA	**0.45**	**0.79**	0.02	0.14	0.16	0.15	-0.02	-0.02	0.16	0.10	0.93
LO-OOA	**0.52**	**0.30**	0.21	0.26	**0.37**	**0.36**	-0.17	0.27	0.04	-0.18	0.88
Sulfur											
TS	0.27	0.06	-0.16	**0.93**	0.10	0.10	-0.03	0.04	-0.01	-0.02	1.00
SO_2	0.11	0.05	-0.14	**0.97**	-0.06	0.06	-0.05	0.05	0.01	-0.05	0.99
TRS	**0.64**	0.01	-0.12	0.11	**0.63**	0.20	0.09	-0.04	-0.09	0.12	0.91
Other											
IVOCs	0.28	**0.50**	0.22	-0.07	**0.66**	0.08	-0.13	0.04	0.06	-0.18	0.87
NH_3	0.00	0.22	-0.20	-0.07	-0.03	0.03	**0.92**	0.11	0.02	-0.06	0.96
CH_4	**0.64**	**0.43**	0.15	-0.07	0.09	0.10	0.00	-0.07	0.17	**0.50**	0.92
Mixing height	-0.04	-0.07	**-0.35**	0.07	0.01	0.00	0.12	**0.90**	0.04	-0.07	0.96
Eigenvalues	6.06	3.81	3.51	2.16	1.19	1.12	1.03	1.02	0.94	0.92	
% var.	26.35	16.57	15.27	9.39	5.19	4.86	4.48	4.42	4.08	3.98	
% Cum. var.	26.35	42.92	58.19	67.58	72.77	77.63	82.11	86.53	90.61	94.60	

Table S-10. The pattern without aerosol variables after Varimax rotation with 9 components.

	1	2	3	4	5	6	7	8	9	Commu-nalities
Anthropogenic VOCs										
o-xylene	**0.88**	0.02	0.04	0.09	0.12	0.10	-0.03	0.17	**0.32**	0.94
1,2,3 - TMB	**0.94**	0.07	0.12	0.04	0.11	0.03	-0.02	0.18	-0.02	0.95
1,2,4 - TMB	**0.94**	0.01	0.11	0.10	0.08	0.08	-0.02	0.19	0.13	0.98
decane	**0.93**	-0.01	0.20	0.16	0.01	0.18	0.04	0.04	0.06	0.97
undecane	**0.89**	-0.07	0.26	0.25	-0.03	0.12	0.06	-0.04	-0.03	0.94
Biogenic VOCs										
α-pinene	-0.03	**0.97**	-0.08	-0.12	0.06	0.01	-0.08	0.02	0.00	0.98
ß-pinene	-0.02	**0.97**	-0.08	-0.12	0.05	0.00	-0.08	0.00	0.01	0.98
limonene	0.08	**0.92**	-0.04	-0.08	0.27	0.10	-0.11	0.03	-0.06	0.95
Combustion tracers										
NO_y	0.30	-0.25	**0.81**	0.23	-0.03	0.24	0.09	-0.06	0.03	0.92
rBC	**0.34**	0.04	**0.78**	0.08	0.12	**0.37**	0.11	0.13	-0.04	0.92
CO	**0.42**	0.04	0.16	0.03	0.10	0.05	0.05	**0.87**	-0.01	0.98
CO_2	0.10	**0.46**	0.06	-0.10	**0.84**	-0.02	-0.13	0.06	-0.05	0.96
Aerosol species										
pPAH	0.07	-0.07	**0.94**	-0.13	0.08	-0.06	0.11	0.12	0.03	0.95
Sulfur										
TS	0.26	-0.15	0.03	**0.94**	-0.05	0.03	-0.02	0.01	0.14	1.00
SO_2	0.12	-0.14	0.02	**0.98**	-0.05	-0.03	-0.03	0.02	-0.04	0.99
TRS	**0.59**	-0.07	0.04	0.14	-0.01	0.19	0.02	-0.02	**0.75**	0.97
Other										
IVOCs	**0.35**	0.13	**0.32**	-0.03	0.00	**0.84**	-0.03	0.05	0.15	0.98
NH_3	0.01	-0.23	0.21	-0.05	-0.10	-0.01	**0.94**	0.05	0.01	1.00
CH_4	**0.61**	0.09	**0.36**	-0.05	**0.59**	0.08	0.00	0.18	0.16	0.92
Eigenvalues	5.54	3.16	2.60	2.08	1.20	1.03	0.97	0.94	0.77	
% var.	29.15	16.63	13.68	10.96	6.33	5.40	5.11	4.96	4.03	
% Cum. var.	29.15	45.79	59.46	70.43	76.76	82.16	87.26	92.23	96.25	

448 **Table S-11.** Criteria for number of components extracted by PCA.

Criterion	Number of components extracted	% Variance explained (after rotation)
Scree test 1	5	81.0%
< 5% variance	6	85.2%
Latent root	7	88.7%
≥ 95% cumulative variance	10	95.5%
Scree test 2	11	96.9%

449

450

451 **Table S-12.** Association of IVOCs with relevant components.

# of components in solution	Oil sands surface mining facilities (Component 1)	Mine fleet and operations (Component 2)	Mine face (Component 5)
5	0.47	0.61	n/a
6	0.31	0.43	n/a
7	0.32	0.48	0.66
8	0.35	0.43	0.71
9	0.32	0.41	0.70
10	0.31	0.39	0.74
11	0.34	0.37	n/a

452

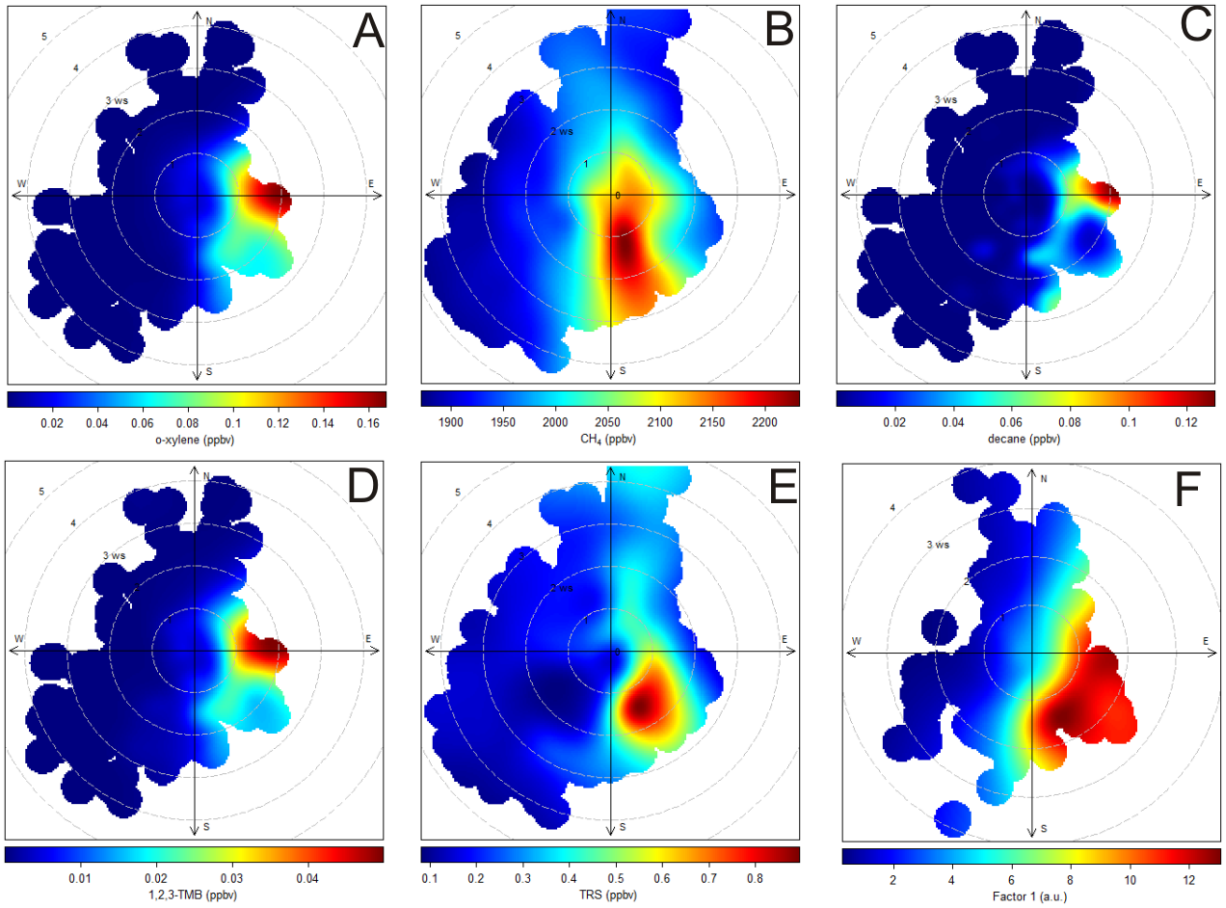

Figure S-3. Bivariate polar plots associated with component 1 for the optimum primary pollutant solution (Table 5.). **(A)** o-xylene, **(B)** CH_4, **(C)** decane, **(D)** 1, 2, 3-TMB, **(E)** TRS, **(F)** and component 1.

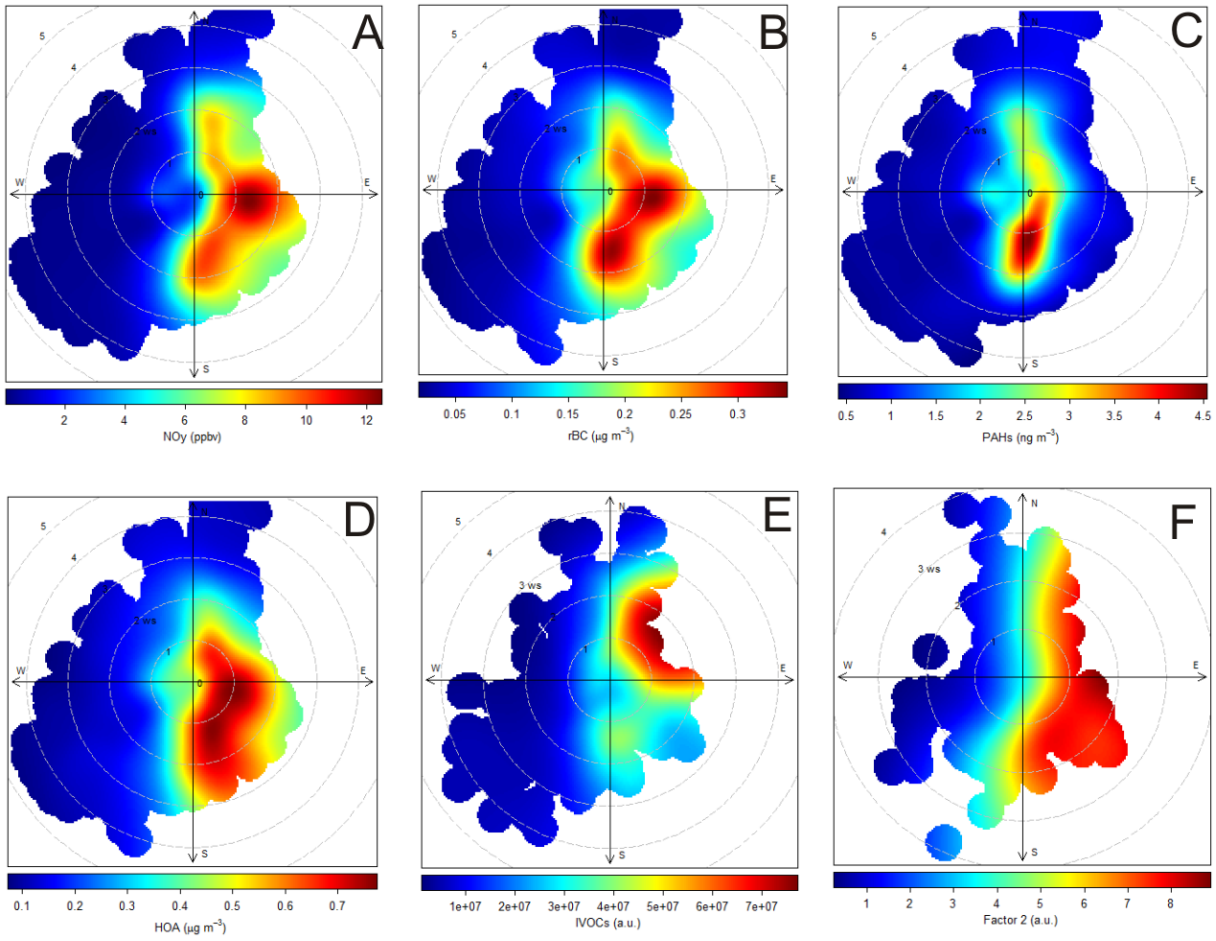

Figure S-4. Bivariate polar plots associated with component 2 for the optimum primary pollutant solution (Table 5.). **(A)** NO_y, **(B)** rBC, **(C)** PAHs, **(D)** HOA, **(E)** IVOCs, **(F)** and component 2.

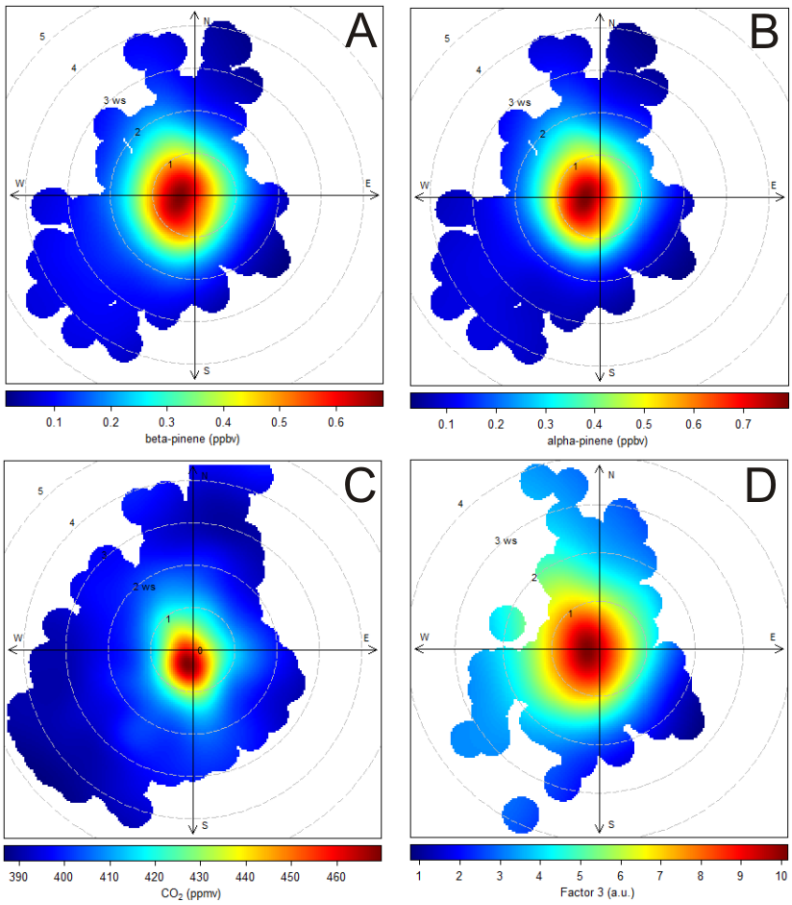

Figure S-5. Bivariate polar plots associated with component 3 for the optimum primary pollutant solution (Table 5.). **(A)** ß-pinene, **(B)** α-pinene, **(C)** CO_2, **(D)** and component 3.

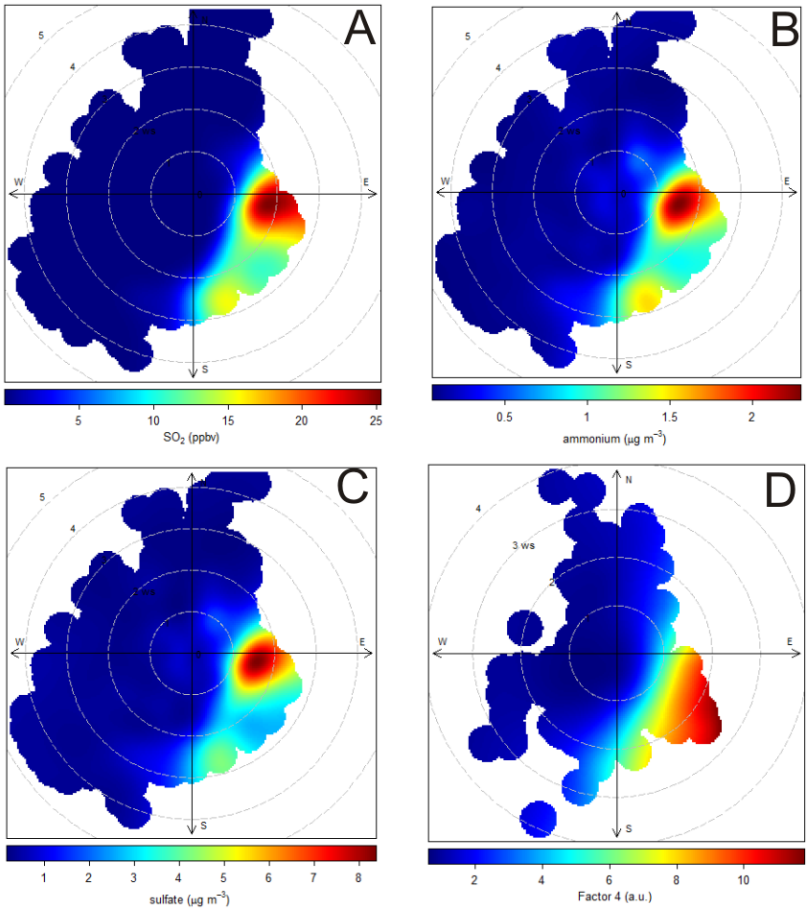

Figure S-6. Bivariate polar plots associated with component 4 for the optimum secondary pollutant solution (Table 7). **(A)** SO_2, **(B)** $NH_4^+{}_{(p)}$, **(C)** $SO_4^{2-}{}_{(p)}$, **(D)** and component 4.

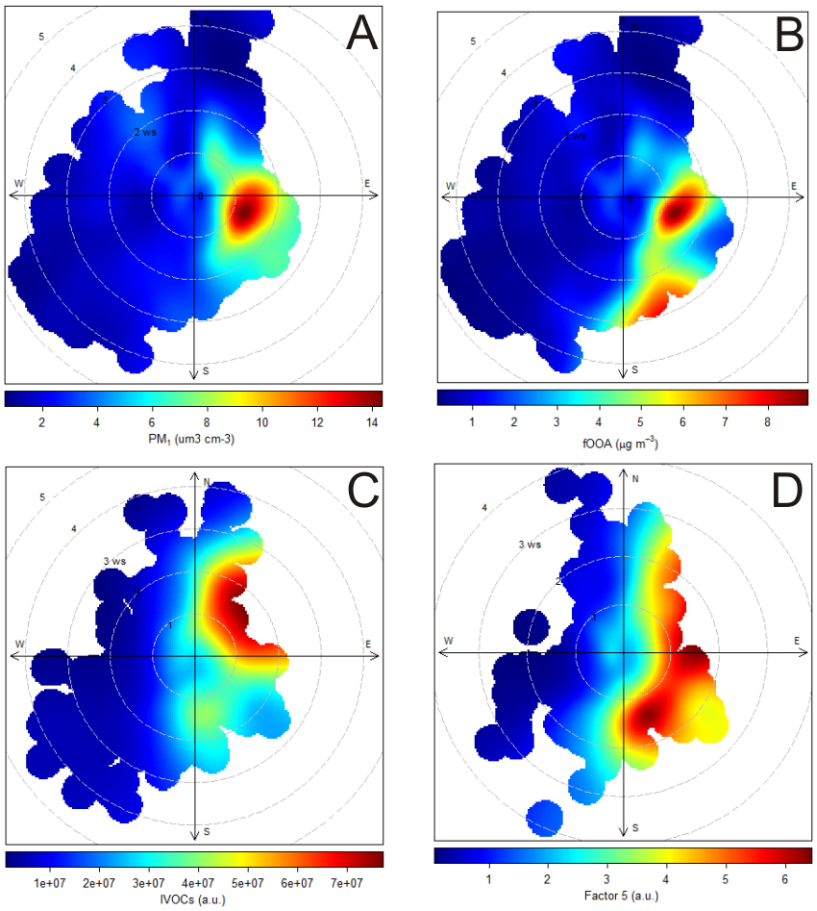

Figure S-7. Bivariate polar plots associated with component 5 for the optimum secondary pollutant solution (Table 7). **(A)** PM_1 (11-component solution), **(B)** LO-OOA, **(C)** IVOCs, and **(D)** component 5.

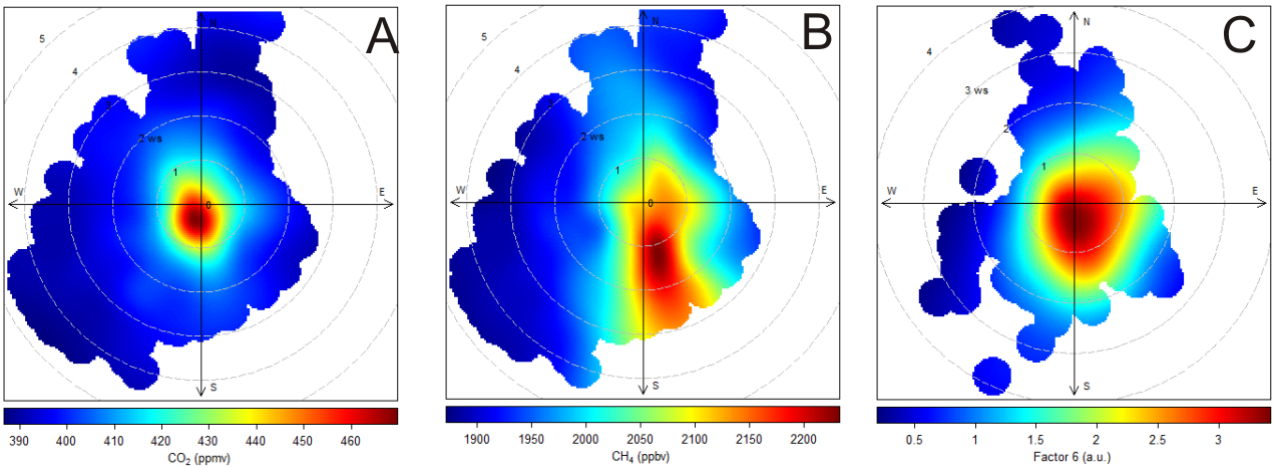

Figure S-8. Bivariate polar plots associated with component 6 for the optimum primary pollutant solution (Table 5). **(A)** CO_2, **(B)** CH_4, and **(C)** component 6.

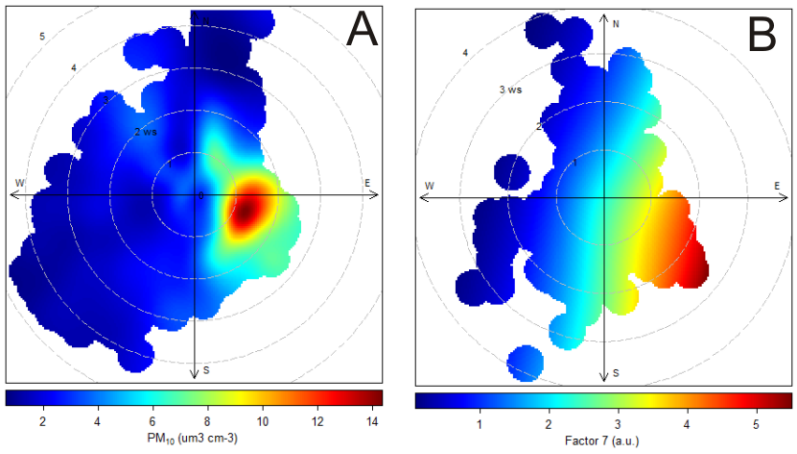

Figure S-9. Bivariate polar plots associated with component 7 for the optimum primary pollutant solution (Table 5). **(A)** PM_{10-1}, **(B)** and component 7.

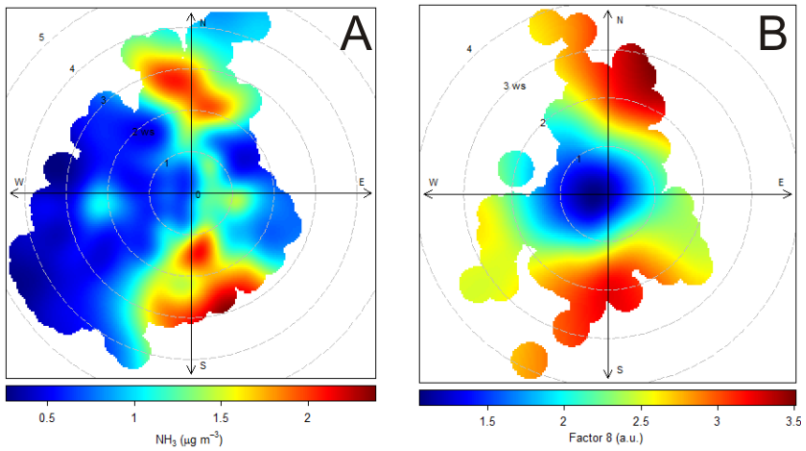

Figure S-10. Bivariate polar plots associated with component 8 for the optimum primary pollutant solution (Table 5). **(A)** NH_3, **(B)** and component 8.

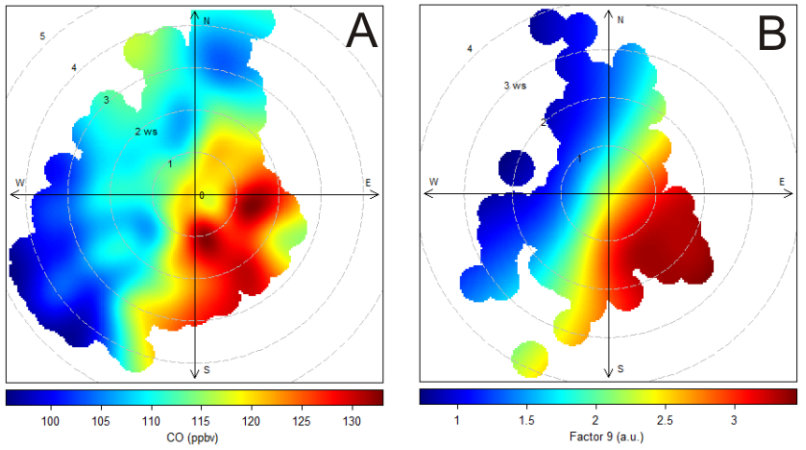

Figure S-11. Bivariate polar plots associated with component 9 for the optimum primary pollutant solution (Table 5). **(A)** CO, and **(B)** component 9.

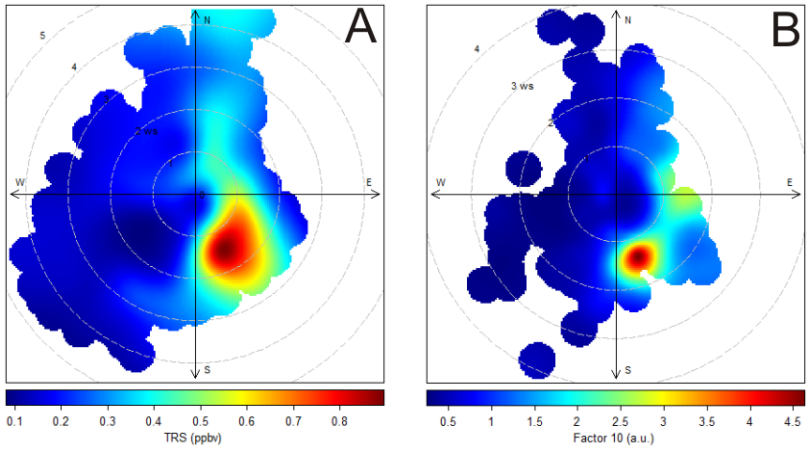

Figure S-12. Bivariate polar plots associated with component 10 for the optimum primary pollutant solution (Table 5). **(A)** TRS, **(B)** and component 10.

Estimate of photochemical age

Photochemical age was calculated using the method outlined by Borbon et al. (2013), but substituting n-decane for benzene since the latter was not quantified. The photochemical age of an air mass, Δt was calculated from the observed concentrations of 124-trimethylbenzene (124TMB) and n-decane using:

$$\Delta t = \frac{1}{[OH]\times(k_{124TMB}-k_{decane})} \times \left[\ln\left(\frac{[124TMB]}{[decane]}\right)_{t=0} - \ln\left(\frac{[124TMB]}{[decane]}\right)\right] \quad \text{(S-1)}$$

where k_{124TMB} = 3.25×10^{-11} cm^3 molecule^{-1} s^{-1} and k_{decane} = 1.10×10^{-11} cm^3 molecule^{-1} s^{-1} are rate coefficients for reaction of OH with 124-TMB and n-decane (at 298 K), respectively, whose values were taken from Seinfeld and Pandis (2006). The ratio of [124TMB] to [decane] at the point of emission (time t = 0) was estimated from a plot of [124TMB] to [n-decane] (Figure S-13, left-hand side) and a straight-line fit to the nocturnal data (assumed to be unaffected by oxidation and shown in blue color). The slope of this line was 1.15±0.07 (r^2 = 0.84). Daytime data (color-coded by solar zenith angle, SZA) exhibit lower ratios of [124TMB]/[decane] as a result of the faster oxidation of 124TMB by OH.

Shown in Figure S-13 on the right-hand side is a plot of the photochemical age, calculated using equation (S-1) and an assumed [OH] of 7×10^6 molecules cm^{-3} taken from Liggio et al. (2016), as a function of SZA (filtered for peak OH of 11:00 and 16:00 local time). The error bars indicate ages calculated using emission factors of 1.08 and 1.22, respectively. The average (±1 standard deviation) photochemical age is 1.0±0.4 hr. This photochemical age applies mainly to component 1; we assume that the photochemical ages of sources associated with other components were similar.

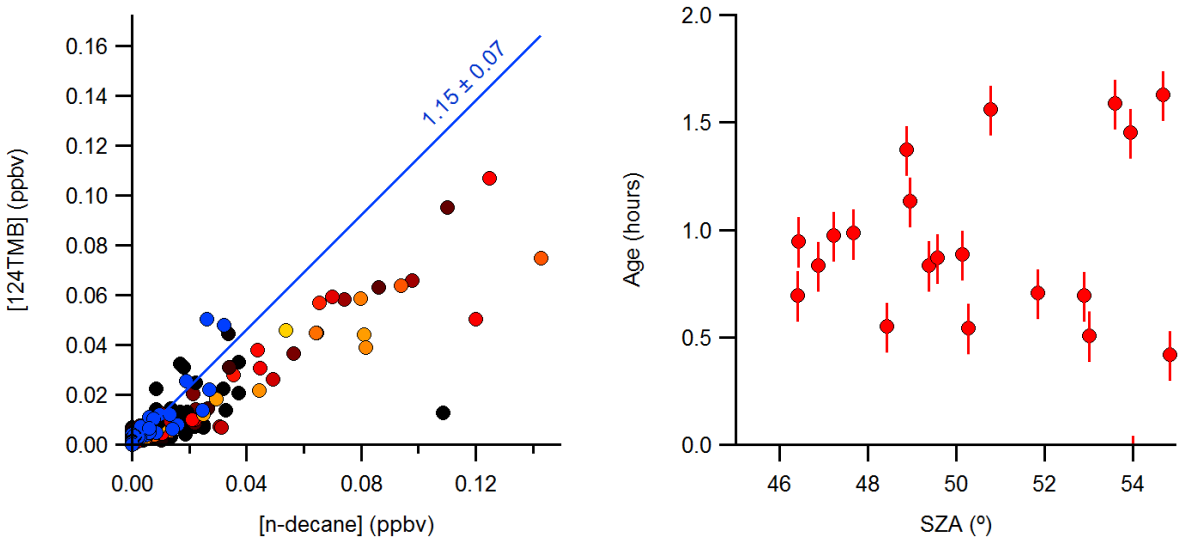

Figure S-13. (A) Plot of 124TMB mixing ratios against mixing ratios of n-decane, color-coded by solar zenith angle. The blue data points were collected at night. **(B)** Photochemical age calculating using equation S-1 plotted as a function of solar zenith angle.

In their analysis of IVOC photochemical aging, Zhao et al. (2014) estimated an average k_{OH} for diesel-exhaust IVOCs of 1.8×10^{-11} cm^3 $molecule^{-1}$ s^{-1} (though their estimated rate coefficients varied and increased slightly with volatility bin between about 1 and 3 $\times10^{-11}$ cm^3 $molecule^{-1}$ s^{-1}). From this, we calculate a pseudo first-order lifetime of 130 min (2.17 hr) with respect to IVOC oxidation by OH during daytime. Using a photochemical age of 1.0±0.4 hr, we calculate that between 25% and 50% of the emitted IVOC is (potentially) oxidized during daytime. Photochemical aging will affect data collected during the daytime hours (from ~11 am to ~4 pm) or ~25% of the data (56 out of 218 data points) used in the PCA and likely resulted in partial conversion of IVOCs to SOA.

References

Borbon, A., Gilman, J. B., Kuster, W. C., Grand, N., Chevaillier, S., Colomb, A., Dolgorouky, C., Gros, V., Lopez, M., Sarda-Esteve, R., Holloway, J., Stutz, J., Petetin, H., McKeen, S., Beekmann, M., Warneke, C., Parrish, D. D., and de Gouw, J. A.: Emission ratios of anthropogenic volatile organic compounds in northern mid-latitude megacities: Observations versus emission inventories in Los Angeles and Paris, J. Geophys. Res.-Atmos., 118, 2041-2057, doi:10.1002/jgrd.50059, 2013.

Bradford, L. M., Ziolkowski, L. A., Goad, C., Warren, L. A., and Slater, G. F.: Elucidating carbon sources driving microbial metabolism during oil sands reclamation, Journal of Environmental Management, 188, 246-254, 10.1016/j.jenvman.2016.11.029, 2017.

Burtscher, H., Scherrer, L., Siegmann, H. C., Schmidtott, A., and Federer, B.: Probing aerosols by photoelectric charging, J. Appl. Phys., 53, 3787-3791, 10.1063/1.331120, 1982.

Bytnerowicz, A., Fraczek, W., Schilling, S., and Alexander, D.: Spatial and temporal distribution of ambient nitric acid and ammonia in the Athabasca Oil Sands Region, Alberta, J. Limnol., 69, 11-21, 10.3274/jl10-69-s1-03, 2010.

Cattell, R. B.: The Scree Test For The Number Of Factors, Multivariate Behavioral Research, 1, 245-276, 10.1207/s15327906mbr0102_10, 1966.

Chen, H., Karion, A., Rella, C. W., Winderlich, J., Gerbig, C., Filges, A., Newberger, T., Sweeney, C., and Tans, P. P.: Accurate measurements of carbon monoxide in humid air using the cavity ring-down spectroscopy (CRDS) technique, Atmos. Meas. Tech., 6, 1031-1040, 10.5194/amt-6-1031-2013, 2013.

ECCC: Measurement instrumentation: carbon dioxide: https://www.ec.gc.ca/mges-ghgm/default.asp?lang=En&n=7903528C-1, access: April 25, 2017, 2013a.

ECCC: National pollutant release inventory (NPRI): http://open.canada.ca/data/en/dataset/e40099ae-b116-4c48-9475-f3806fe5a6a6, access: October 5, 2016, 2013b.

Gorham, E.: Northern peatlands - role in the carbon-cycle and probable responses to climatic warming, Ecol. Appl., 1, 182-195, 10.2307/1941811, 1991.

Hair, J. F., Anderson, R. E., Tatham, R. L., and Black, W. C.: Multivariate data analysis, in, 7th edition ed., Prentice-Hall, Upper Saddle River, NJ, pp. 108 -110, 1998.

Holowenko, F. M., MacKinnon, M. D., and Fedorak, P. M.: Methanogens and sulfate-reducing bacteria in oil sands fine tailings waste, Canadian Journal of Microbiology, 46, 927-937, 10.1139/cjm-46-10-927, 2000.

Huffman, J. A., Treutlein, B., and Pöschl, U.: Fluorescent biological aerosol particle concentrations and size distributions measured with an Ultraviolet Aerodynamic Particle Sizer (UV-APS) in Central Europe, Atmos. Chem. Phys., 10, 3215-3233, 10.5194/acp-10-3215-2010, 2010.

Johnson, M. R., Crosland, B. M., McEwen, J. D., Hager, D. B., Armitage, J. R., Karimi-Golpayegani, M., and Picard, D. J.: Estimating fugitive methane emissions from oil sands mining using extractive core samples, Atmos. Environm., 144, 111-123, 10.1016/j.atmosenv.2016.08.073, 2016.

Liggio, J., Li, S.-M., Hayden, K., Taha, Y. M., Stroud, C., Darlington, A., Drollette, B. D., Gordon, M., Lee, P., Liu, P., Leithead, A., Moussa, S. G., Wang, D., O'Brien, J., Mittermeier, R. L., Brook, J., Lu, G., Staebler, R., Han, Y., Tokarek, T. W., Osthoff, H. D., Makar, P. A., Zhang, J., Plata, D., and Gentner, D. R.: Oil Sands Operations as a Large Source of Secondary Organic Aerosols, Nature, 534, 91-94, 10.1038/nature17646, 2016.

Marey, H. S., Hashisho, Z., Fu, L., and Gille, J.: Spatial and temporal variation in CO over Alberta using measurements from satellites, aircraft, and ground stations, Atmos. Chem. Phys., 15, 3893-3908, 10.5194/acp-15-3893-2015, 2015.

Markovic, M. Z., VandenBoer, T. C., and Murphy, J. G.: Characterization and optimization of an online system for the simultaneous measurement of atmospheric water-soluble constituents in the gas and particle phases, J. Environ. Monit., 14, 1872-1884, 10.1039/C2EM00004K, 2012.

584 Miller, S. M., Worthy, D. E. J., Michalak, A. M., Wofsy, S. C., Kort, E. A., Havice, T. C., Andrews, A. E.,
585 Dlugokencky, E. J., Kaplan, J. O., Levi, P. J., Tian, H. Q., and Zhang, B. W.: Observational constraints on
586 the distribution, seasonality, and environmental predictors of North American boreal methane
587 emissions, Glob. Biogeochem. Cycle, 28, 146-160, 10.1002/2013gb004580, 2014.
588 Nara, H., Tanimoto, H., Tohjima, Y., Mukai, H., Nojiri, Y., Katsumata, K., and Rella, C. W.: Effect of air
589 composition (N_2, O_2, Ar, and H_2O) on CO_2 and CH_4 measurement by wavelength-scanned cavity ring-
590 down spectroscopy: calibration and measurement strategy, Atmos. Meas. Tech., 5, 2689-2701,
591 10.5194/amt-5-2689-2012, 2012.
592 NPRI: Detailed facility information: http://www.ec.gc.ca/inrp-npri/donnees-
593 data/index.cfm?do=facility_information&lang=En&opt_npri_id=0000002274&opt_report_year=2013
594 , access: April 13, 2017, 2013.
595 Nwaishi, F., Petrone, R. M., Macrae, M. L., Price, J. S., Strack, M., and Andersen, R.: Preliminary
596 assessment of greenhouse gas emissions from a constructed fen on post-mining landscape in the
597 Athabasca oil sands region, Alberta, Canada, Ecol. Eng., 95, 119-128, 10.1016/j.ecoleng.2016.06.061,
598 2016.
599 Odame-Ankrah, C. A.: Improved detection instrument for nitrogen oxide species, Ph.D., Chemistry,
600 University of Calgary, http://hdl.handle.net/11023/2006, 10.5072/PRISM/26475, Calgary, 2015.
601 Oertel, C., Matschullat, J., Zurba, K., Zimmermann, F., and Erasmi, S.: Greenhouse gas emissions from
602 soils A review, Chem Erde-Geochem., 76, 327-352, 10.1016/j.chemer.2016.04.002, 2016.
603 Onasch, T. B., Trimborn, A., Fortner, E. C., Jayne, J. T., Kok, G. L., Williams, L. R., Davidovits, P., and
604 Worsnop, D. R.: Soot Particle Aerosol Mass Spectrometer: Development, Validation, and Initial
605 Application, Aerosol Sci. Technol., 46, 804-817, 10.1080/02786826.2012.663948, 2012.
606 Percy, K. E.: Ambient Air Quality and Linkage to Ecosystems in the Athabasca Oil Sands, Alberta, Geosci.
607 Can., 40, 182-201, 10.12789/geocanj.2013.40.014, 2013.

608 Phillips-Smith, C., Jeong, C. H., Healy, R. M., Dabek-Zlotorzynska, E., Celo, V., Brook, J. R., and Evans, G.:
609 Sources of Particulate Matter in the Athabasca Oil Sands Region: Investigation through a Comparison
610 of Trace Element Measurement Methodologies, Atmos. Chem. Phys. Discuss., 2017, 1-34,
611 10.5194/acp-2016-966, 2017.
612 Quagraine, E. K., Headley, J. V., and Peterson, H. G.: Is biodegradation of bitumen a source of recalcitrant
613 naphthenic acid mixtures in oil sands tailing pond waters?, J. Environ. Sci. Health Part A-Toxic/Hazard.
614 Subst. Environ. Eng., 40, 671-684, 10.1081/ese-200046637, 2005.
615 Rooney, R. C., Bayley, S. E., and Schindler, D. W.: Oil sands mining and reclamation cause massive loss of
616 peatland and stored carbon, Proc. Natl. Acad. Sci. U.S.A., 109, 4933-4937, 10.1073/pnas.1117693108,
617 2012.
618 Seinfeld, J. H., and Pandis, S. N.: Atmospheric chemistry and physics: from air pollution to climate
619 change, 2nd ed., Wiley, Hoboken, N.J., 2006.
620 Shephard, M. W., McLinden, C. A., Cady-Pereira, K. E., Luo, M., Moussa, S. G., Leithead, A., Liggio, J.,
621 Staebler, R. M., Akingunola, A., Makar, P., Lehr, P., Zhang, J., Henze, D. K., Millet, D. B., Bash, J. O.,
622 Zhu, L., Wells, K. C., Capps, S. L., Chaliyakunnel, S., Gordon, M., Hayden, K., Brook, J. R., Wolde, M.,
623 and Li, S. M.: Tropospheric Emission Spectrometer (TES) satellite observations of ammonia,
624 methanol, formic acid, and carbon monoxide over the Canadian oil sands: validation and model
625 evaluation, Atmospheric Measurement Techniques, 8, 5189-5211, 10.5194/amt-8-5189-2015, 2015.
626 Small, C. C., Cho, S., Hashisho, Z., and Ulrich, A. C.: Emissions from oil sands tailings ponds: Review of
627 tailings pond parameters and emission estimates, Journal of Petroleum Science and Engineering, 127,
628 490-501, 10.1016/j.petrol.2014.11.020, 2015.
629 Thompson, R. L., Sasakawa, M., Machida, T., Aalto, T., Worthy, D., Lavric, J. V., Myhre, C. L., and Stohl, A.:
630 Methane fluxes in the high northern latitudes for 2005-2013 estimated using a Bayesian atmospheric
631 inversion, Atmos. Chem. Phys., 17, 3553-3572, 10.5194/acp-17-3553-2017, 2017.

632 Tokarek, T. W., Huo, J. A., Odame-Ankrah, C. A., Hammoud, D., Taha, Y. M., and Osthoff, H. D.: A gas
633 chromatograph for quantification of peroxycarboxylic nitric anhydrides calibrated by thermal
634 dissociation cavity ring-down spectroscopy, Atmos. Meas. Tech., 7, 3263-3283, 10.5194/amt-7-3263-
635 2014, 2014.
636 Tokarek, T. W., Brownsey, D. K., Jordan, N., Garner, N. M., Ye, C. Z., Assad, F. V., Peace, A., Schiller, C. L.,
637 Mason, R. H., Vingarzan, R., and Osthoff, H. D.: Biogenic Emissions and Nocturnal Ozone Depletion
638 Events at the Amphitrite Point Observatory on Vancouver Island, Atmosphere-Ocean, 1-12,
639 10.1080/07055900.2017.1306687, 2017.
640 Wang, X. L., Chow, J. C., Kohl, S. D., Percy, K. E., Legge, A. H., and Watson, J. G.: Characterization of
641 PM2.5 and PM10 fugitive dust source profiles in the Athabasca Oil Sands Region, J. Air Waste Manag.
642 Assoc., 65, 1421-1433, 10.1080/10962247.2015.1100693, 2015.
643 Warner, D. L., Villarreal, S., McWilliams, K., Inamdar, S., and Vargas, R.: Carbon Dioxide and Methane
644 Fluxes From Tree Stems, Coarse Woody Debris, and Soils in an Upland Temperate Forest, Ecosystems,
645 10.1007/s10021-016-0106-8, 2017.
646 Warren, L. A., Kendra, K. E., Brady, A. L., and Slater, G. F.: Sulfur Biogeochemistry of an Oil Sands
647 Composite Tailings Deposit, Front. Microbiol., 6, 14, 10.3389/fmicb.2015.01533, 2016.
648 Wesely, M. L., and Hicks, B. B.: A review of the current status of knowledge on dry deposition, Atmos.
649 Environm., 34, 2261-2282, 10.1016/S1352-2310(99)00467-7, 2000.
650 Whalen, S. C.: Biogeochemistry of methane exchange between natural wetlands and the atmosphere,
651 Environ. Eng. Sci., 22, 73-94, 10.1089/ees.2005.22.73, 2005.
652 Whaley, C. H., Makar, P. A., Shephard, M. W., Zhang, L., Zhang, J., Zheng, Q., Akingunola, A., Wentworth,
653 G. R., Murphy, J. G., Kharol, S. K., and Cady-Pereira, K. E.: Contributions of natural and anthropogenic
654 sources to ambient ammonia in the Athabasca Oil Sands and north-western Canada, Atmos. Chem.
655 Phys., 18, 2011-2034, 10.5194/acp-18-2011-2018, 2018.

656 Wilson, N. K., Barbour, R. K., Chuang, J. C., and Mukund, R.: Evaluation of a real-time monitor for fine
657 particle-bound PAH in air, Polycycl. Aromat. Compd., 5, 167-174, 10.1080/10406639408015168,
658 1994.
659 Yavitt, J. B., Williams, C. J., and Wieder, R. K.: Soil chemistry versus environmental controls on
660 production of CH_4 and CO_2 in northern peatlands, Eur. J. Soil Sci., 56, 169-178, 10.1111/j.1365-
661 2389.2004.00657.x, 2005.
662 Zhang, L. M., Brook, J. R., and Vet, R.: On ozone dry deposition - with emphasis on non-stomatal uptake
663 and wet canopies, Atmos. Environm., 36, 4787-4799, 10.1016/s1352-2310(02)00567-8, 2002.
664 Zhao, Y. L., Hennigan, C. J., May, A. A., Tkacik, D. S., de Gouw, J. A., Gilman, J. B., Kuster, W. C., Borbon,
665 A., and Robinson, A. L.: Intermediate-Volatility Organic Compounds: A Large Source of Secondary
666 Organic Aerosol, Environm. Sci. Technol., 48, 13743-13750, 10.1021/es5035188, 2014.
667
668